Forecasting Research Division

Technical Report No. 39

Performance of the data assimilation scheme in the operational trial of the new mesoscale model

by

B Macpherson, B J Wright and A J Maycock

February 1993

FORECASTING RESEARCH TECHNICAL REPORT NO 39

Performance of the data assimilation scheme in the operational trial of the new mesoscale model

by

B Macpherson, B J Wright and A J Maycock

February 1993

ABSTRACT

The formulation of the assimilation scheme for the new mesoscale model (NMM) is described, along with differences between the NMM and its predecessor (the OMM) in qualitative behaviour and objective verification early in the forecast. The NMM does not suffer like the OMM from excessive early convection or loss of grid-scale cloud. The NMM does not fit data so closely as the OMM at analysis time, but by t+3 or t+6 both models verify similarly for a range of variables. Screen temperature errors in the NMM tend to decrease in the first 6 hours of the forecast, especially through the decay of an initial cold bias on winter mornings.

MOPS cloud data in the NMM are of benefit to rainfall forecasts mainly in the first 6 hours, and give improved cloud cover (and to a lesser extent cloud base), especially in a stratocumulus situation. They also contribute indirectly to better screen temperature forecasts, although the direct impact of screen temperature data is slightly greater, and may last until t+18-24 in anticyclonic situations.

An error in the preparation of MOPS cloud data for model level 1 in the NMM's operational trial caused a moist bias in screen level humidity early in the forecast and spurious fog formation in the stratocumulus case. Reruns with the error corrected show substantial improvement.

Forecasting Research Division,
Meteorological Office,
London Road,
Bracknell,
Berkshire RG12 2SZ,
United Kingdom.

1. Introduction

The new mesoscale model (NMM), a version of the unified model (Cullen 1991), became operational on 8th December 1992, replacing a system which we shall refer to as the old mesoscale model (OMM), described by Golding (1990). Operational implementation followed a preliminary trial in spring 1992 and an operational trial in autumn 1992, the results of which are reported here. This second trial of the NMM examined model performance in 9 cases (listed in Appendix B) chosen to cover a variety of situations of 'mesoscale interest.' This report summarises differences in performance between the assimilation schemes of the old and new models and examines the impact on forecast accuracy from assimilating particular types of data in the NMM. For a companion paper to this one on the forecast model as a whole, see Ballard and Robinson (1993). We begin with a review of the assimilation formulation. A summary of the NMM forecast model formulation is given in Appendix A.

2. Formulation

The Interactive Mesoscale Initialisation (IMI) for the OMM (Wright and Golding 1990) is explained schematically in Figure 1. The assimilation scheme for the new model is outlined in Figure 2.

The main difference between the two schemes is assimilation *technique*. In the IMI/OMM, analysed fields were imposed on the model *instantaneously* (ie at one time level t+0) as initial conditions. In the NMM, the data are assimilated *continuously* over two 3-hour cycles of mesoscale model integration, using the Analysis Correction scheme (Lorenc, Bell and Macpherson 1991) as in the Limited Area Model (LAM) and global model. As in the LAM, data assimilation in the NMM actually ceases at t+2 into the forecast run. The 'nudging' coefficient, which determines the rate of adjustment of the model towards observations, has the same value in the NMM as in the LAM.

2.1 Upper-air data

In the NMM, radiosondes are assimilated directly at the NMM vertical resolution. Other upper-air observations such as aireps, satellite temperature soundings and CFO bogus data are also assimilated directly. The OMM relied on interpolation of a coarser resolution LAM analysis for upper-air structure, although the IMI did allow a forecaster to modify vertical temperature and cloud profiles interactively. Treatment in the NMM of moisture data other than radiosondes is described in Sections 2.3-2.5.

Assimilation parameters such as the model background error correlation scales and the radii of influence of observations have the same values in the NMM as in the LAM for upper-air data.

2.2 Surface data

The surface data assimilated by the NMM are hourly screen temperature (synop but not ship), synop wind, ship wind and surface pressure data. The OMM/IMI analysed these data 3-hourly. CFO bogus data are also passed to

the new model. Note that screen temperature and synop wind data are not used in the LAM, which also receives only 3-hourly surface pressure data.

Screen level dew point data were analysed in the IMI, but are *not yet* assimilated operationally by the NMM, although it is planned to introduce them into the new model in mid-1993. Also, the IMI performed a separate visibility analysis which is not included in the new system. It is anticipated that surface humidity data will have an impact on visibility prediction. (It is also possible to influence visibility in the model through the Moisture Observation Pre-processing System, see Section 2.4).

Screen temperature data input to the NMM are corrected (before quality control) by a standard lapse rate for differences between station and model orographic height. This was not done in the OMM/IMI. The screen temperature data increments are applied to the NMM surface temperature T_* and with decreasing weight in the vertical up to a height of approximately 600m (model level 6). The T_* increment is applied only at land points; no change is made to the sea surface temperature.

Synop wind data increments are computed with respect to a model background wind field derived at 10m. As in the global model and LAM, ship wind observations are assumed to have a nominal height of 20m, and are compared with a model field at level 1, approximately 25m. The vertical spreading of increments from all surface wind data is as for screen temperature data.

A *station blacklist* exists for synop wind data, so that certain high level or valley stations are not used where they are considered unrepresentative of the mesoscale gridbox. This blacklist was compiled by comparing observations for several months against the LAM 10m wind, and will be refined when an Observation Processing Database (OPD) is available for the NMM.

The NMM *assimilation parameters* for surface data have been tuned relative to LAM values to improve the analysis of small scales. The model background error correlation scale for surface data is currently set to 150km, and the data are not used beyond an influence radius of approximately 260km. The insertion period for data in the LAM is 2·5 hours before valid time and 0·5 hours after valid time. In the NMM, these values were reduced by 20% for surface data to 2 hours before and 0·4 hours after observation time. With the change from 3-hourly to hourly data supply for the NMM, the option of an insertion period as short as one hour was considered, but in practice only a subset of stations report hourly. In areas where the reports are 3-hourly, a very short insertion period would give insufficient time for the model to adjust towards the data. The values selected are a compromise.

Observation errors assumed for surface data are 1mb for p_*, 2K for screen temperature and 2ms^{-1} for each wind component. It should be remembered that these are not purely instrument errors, but include the error of representativeness which accounts for the fact that an accurate local measurement may contain information in scales not resolved by the model. The assimilation scheme will tend to fit data roughly to within these assumed errors, which will be updated once statistics are available from the OPD.

2.3 Moisture Observation Pre-processing System (MOPS)

In the Moisture Observation Pre-processing System (MOPS) shown in Figure 3, a *3-d cloud fraction analysis* is prepared with interactive supervision, in a manner similar to the corresponding parts of the IMI. Like the IMI, MOPS is a menu driven system, controlled by 'mouse' input (and keyboard where required), which is operated by the forecaster on an interactive graphics workstation. For a full account of MOPS, refer to Wright (1993). The following are some of the main points.

MOPS comprises a subset of the tasks in the IMI, but focussing on cloud; MOPS omits the analyses of pmsl, 10m wind, visibility, screen temperature and dew point data performed in the IMI, data for which are (or will be) assimilated directly by the NMM.

The precipitation rate analysis is constructed from a combination of the model background field (a 3-hour forecast), the FRONTIERS radar image, present weather reports and hourly accumulations. It is used *only* to provide input to the 3-d cloud analysis.

The first guess for the cloud analysis is again a 3-hour model forecast. Data used in the cloud analysis are as in the IMI. Meteosat IR imagery provides improved cloud cover and cloud top height fields. Surface reports of cloud parameters (including '8-group' reports) give input to the total cloud cover, cloud base height and final multi-level cloud fraction analyses. Meteosat visible and sferics imagery is also available to the forecaster for reference.

2.4 Forecaster intervention in MOPS

The forecaster's main priorities are to detect any corrupt satellite imagery and monitor the cloud cover and cloud top height analyses. Without intervention, these analyses can be grossly in error in situations where, with some straightforward intervention, the greatest benefit can be achieved from the data.

In the *cloud cover* analysis, cloud diagnosis from the Meteosat IR image relies on comparison of the IR brightness temperature with the model surface temperature. If these are similar, as may happen when warm low cloud is present, the pixel may be wrongly diagnosed as cloud free and any cloud correctly present in the model first guess removed. The forecaster can restore this.

Although there is no visibility analysis in MOPS, the cloud cover analysis can be used to force *fog* into the model if it is analysed as shallow cloud with a base at the surface.

In the *cloud top height* analysis, a cloud top temperature derived from satellite imagery is assigned a height based on the model's first guess vertical structure. In the presence of an inversion that is inadequately resolved by the model, often associated with stratocumulus sheets, this procedure may produce gross errors if run automatically. The forecaster can easily set a sensible cloud top height.

Research into *automatic algorithms* to cope with these problems will be pursued, with the prospect of eliminating the need for human intervention in MOPS towards the end of 1993.

2.5 Assimilation of MOPS cloud data

The multi-level cloud fraction analysis output from MOPS is converted into *profiles of relative humidity* at every gridpoint for assimilation by the model as 'pseudo-radiosondes'. This conversion uses a relationship consistent with the model's large scale cloud scheme. The MOPS humidity data are assigned empirical observation errors at each level which are typical of UK radiosondes. Where the analysed MOPS cloud fraction is zero, a special data value is set in the derived profile and used to constrain the model humidity to lie below the threshold for cloud formation. MOPS data are used only in the NMM and not in the LAM.

3. Problems with the IMI and corresponding behaviour in the NMM.

Dynamical imbalance in the OMM initial conditions generated by the IMI leads to two commonly observed deficiencies in the first 3-6 hours of the forecast.

3.1 Excessive early convection

The IMI induces excessive convection in the OMM. For an example, see Figure 4(b) at t+1, where the convection exceeds that present at t+0 and t+3. The NMM, however, has a smoother evolution of rainfall rate, as seen in Figure 4(d,e,f).

3.2 Early loss of grid-scale cloud

During the period of adjustment to the IMI initial data, mixing in the OMM leads to rapid loss of cloud, as seen in the OMM mean cloud error curves in Figure 5. The table below gives the *change* in mean cloud cover error between t+0 and t+3, averaged over all surface stations for the 9 trial cases.

	OMM	NMM	NMM (no MOPS)
Change in mean cloud cover error from t+0->t+3 (oktas)	-1·7	+0·6	+0·04

The NMM shows an opposite signature to the OMM, with a gradual *build up* of cloud over the first 3 hours, which is shown to come mainly from the MOPS cloud assimilation - in extra experiments without MOPS data the mean change in this period is very small (Figure 5).

The initial build up of cloud in the NMM is usually beneficial because, like the OMM, it has a mean deficit of cloud at t+3.

4. Differences in objective verification early in the forecast.

4.1 Screen temperature

The IMI produces a close fit to surface data at t+0 in the OMM and has smaller rms analysis errors than the NMM, as can be seen from the time series of temperature errors in Figure 6. However, the advantage of such a close fit to data is lost within the first 3-6 hours of the forecast as OMM rms errors increase and NMM rms errors often *decrease* over the same period.

fit to data

The NMM assimilation scheme does not attempt to fit the data so closely as the IMI at t+0. Instead, it aims to fit them approximately to within their assigned observational error, which allows for the fact that the local measurement may not be representative of scales resolved by the model. This specified error is currently 2K, which appears to be too large according to statistics on rms difference between observations as a function of station separation (Brian Golding, personal communication). For station separations of around 15km in the UK, a typical rms difference is 1K, which should reflect the combination of instrumental error and error of representativeness for a grid box of side 15km. This figure comes from station pairs in lowland Britain, so may underestimate the error of representativeness in upland areas, but 2K is clearly too high.

From the rms forecast error at t+3 of approximately 1·8K (Figure 6), one can deduce an upper bound for the model background error variance of $(1{\cdot}8^2-1^2)$, which gives an rms error of about 1·5K. This is an upper bound because the verification does not take account of differences between station and model orographic height. Further optimisation of these errors will be possible from OPD statistics once the model is operational.

Since the t+0 rms fit to data is close to 2K, it seems that the NMM assimilation should be tuned to draw more closely to the data. A reduction in specified observation error relative to background error would help in this, but it is likely that a smaller forecast error correlation scale would be more fruitful. OPD studies should be able to produce a better estimate for this parameter and for the observation and background errors.

time evolution of errors

The early decrease in NMM errors is counter to the normal error growth behaviour of assimilation/forecast systems. It is relevant that data assimilation ceases in the NMM only at t+2, but this does not explain the continuing decrease to t+6, especially noticeable in the mean over cases with data time 6Z. These are winter cases, so the behaviour may be due to model errors causing analysis problems at a time of minimum (and low) temperature, while temperatures at t+6 in the middle of the day are less subject to model error.

Support for this comes from a study of the OPD verification statistics for screen temperature from the LAM over the whole month of December 1991, including only UK stations so that the domain is similar to that of the NMM. The LAM does not assimilate screen temperature data, and so its t+0

and t+3 accuracy largely reflects that of the model. The OPD results show a maximum rms error at 6z (both for t+0 and t+3), which decreases by more than one degree by 12z. In particular the t+3 valid at 9z has a smaller error than the t+0 at 6z, as found in some of the NMM cases. This error variation in the LAM is dominated by the decay of a cold bias, a feature true also of the NMM (Figure 7), especially for the 6z cases.

Results in Figure 7 from NMM experiments *without* assimilation of screen temperature data (or MOPS cloud data or 10m wind data over land) show little impact from these data on the time tendency of errors early in the forecast.

There is a possibility that large errors initially result from the reconfiguration of a larger scale (global) field to provide the start field at t-6 for mesoscale data assimilation. This was investigated by choosing a case *since* operational implementation of the NMM which showed similar characteristics to the 6z cases of the trial. The operational 6z assimilation and forecast was then rerun, beginning at 0z from a mesoscale analysis instead of a reconfigured global analysis as is done operationally. The results (Figure 8) show that the early NMM behaviour is not a reflection of the reconfiguration.

It is noticeable that the early behaviour is not repeated 24 hours into the 6z forecasts; there is some warming between t+21 and t+27, but the bias around t+24 is close to zero. One possible reason might be a difference in cloud cover errors between the first and second nights in the forecast. Figure 5 does show a slightly greater deficit of cloud between t+0-t+6 than from t+24-t+30.

4.2 10m wind over land

Similar comments apply regarding fit to synop wind data as for screen temperature data. The OMM/IMI gives a closer fit at t+0, but the impact of this relative to the NMM dies off in 3-6 hours (Figure 9).

4.3 Cloud cover

The IMI gives a slightly closer rms fit to cloud cover data at t+0 than the NMM overall, but by t+3 the NMM has a lower error (Figure 10). The reason for this is cloud loss in the OMM, explained in Section 3.2 above.

4.4 Cloud base

The same IMI problem is reflected in the cloud base height verification at t+0 and t+3 (Figure 11). If observed bases are considered in 3 categories of (0-1000'), (1000-2000'), and (2000-5000'), then the percentage forecast in the correct category from the OMM drops from 70% at t+0 to 21% at t+3. For the NMM, the drop is less rapid, from 57% to 31%. Further into the forecast, the skill level of both models is similar, around 30%.

5. Forecast impact from MOPS cloud data

Extra runs with MOPS data withdrawn from the NMM assimilation (NMM-MOPS) were performed as a data impact study on all 9 trial cases. For some cases, two extra reruns were also carried out: one *with* MOPS data but *without* radiosonde humidity observations (NMM-SONDE RH) and a second with *neither* MOPS *nor* radiosonde humidity data (NMM-ALL RH).

5.1 on precipitation

In terms of subjective impact, the most notable example occurs in the t+3 forecast of thunderstorms on 6/7/91 (Figure 12). The NMM gives a more reasonable orientation than the OMM of the rain band over southern England, much of which is lost in the NMM-MOPS run. The NMM-SONDE RH run (Figure 13) has too much rain over southern England at 3z, so the combination of MOPS and radiosonde data gives better results than either data source alone. The NMM-ALL RH run (Figure 13) gives poor indication of the rain distribution at 3z.

The verification of 6-hour accumulations up to t+6 at 6z, 6/7/91 (Figure 14) is consistent with the 3z rain rate snapshots. The NMM trial run, including MOPS, is the best of the various unified model runs for that period. Removal of either MOPS or radiosonde data gives a significant drop in skill. In the next 6-hour period there is negligible signal from MOPS, but omission of radiosondes does reduce skill noticeably. The later NMM evolution error, also present in the OMM, was not corrected by inclusion of MOPS data.

In a second case DT 6z, 8/11/91 (Figure 14), there is detectable benefit from MOPS data in accumulations throughout t+0-t+24, but particularly from t+6-t+12. In this period, the run with MOPS data but no radiosonde data is better than the run with both. In a further two trial cases with substantial precipitation (23/8/91 and 17/2/92), there was little consistent impact from MOPS.

5.2 on cloud cover

The largest impact from MOPS came in the stratocumulus case, DT 0z, 4/12/91, where Figures 15 and 16 show that the NMM run with MOPS data had a more realistic coverage at t+3 than either the run without MOPS data or the OMM forecast, which suffered from rapid cloud loss after t+0. There is significantly more cloud retained to t+18 with MOPS data included, of benefit to the NMM forecast. On this occasion, the NMM-SONDE RH gives a better 3-hour forecast than the NMM run.

It is important to note that the benefit from MOPS in this case was only achieved with human intervention. Problems with the automatic use of the satellite image required the addition of cloud over land and the reduction of cloud top heights in the low cloud areas. The results from an experiment run with automatically prepared MOPS data (autoMOPS in Figure 17) are much more like those from the NMM-MOPS run than those from the NMM run.

In another case DT 0z, 1/9/91, intervention on cloud base height near the coast of NE England appeared to be responsible for the incorrect

removal by the run with MOPS data of an area of low stratus over land. MOPS data degraded the cloud cover verification at t+3 and t+6.

Objective verification of rms cloud cover shows lower errors overall in the NMM relative to the OMM and confirms benefit from MOPS (Figure 10). The influence of MOPS lasts up to t+15-t+18 overall, but is most persistent in the anticyclonic cases. On a case count basis, considering 9 cases at 6 forecast times from t+3-t+18, the NMM had a lower error than the OMM on 65% of occasions, and a larger error on 30%, with 5% equal. MOPS was beneficial to the NMM run on 65% of occasions, worse on 13% and gave no signal on a further 22%.

5.3 on cloud base

The objective verification in Figure 11 shows that, over all cases, MOPS gives more accurate cloud base heights from t+0-t+6, but that from t+9 onwards the impact is negligible (and there is then little difference between the OMM and NMM).

5.4 on tephigrams

One qualitatively unrealistic feature introduced with MOPS is an inconsistency in the t+0 ascents between the height of the very moist stratocumulus layer as defined mainly by the MOPS data and the temperature inversion structure which results from assimilating radiosondes. Although MOPS (with human intervention) improves the cloud top height (Figure 18), the temperature analysis has not altered very much from that in the run without MOPS data and does not 'match' the moisture profile. There is much better consistency in the ascents by t+6 and the problem is negligible by t+12. The analysed ascent with automatically prepared MOPS data (Figure 18(d)) betrays the problem with cloud top height assignment in MOPS when the model inversion structure in the first guess is unrealistic. The cloud layer at 750mb is spurious.

5.5 on fit to radiosondes

Overall, the analysis with MOPS data does not fit radiosonde humidity data as closely as when MOPS data are omitted. Averaging over the five cases with DT 0z and over all vertical levels, inclusion of MOPS data increases the bias of the model relative to radiosondes from +0·2% to +2·2% and the rms fit is degraded from 11·9% to 12·3%. In two cases, however, MOPS led to a closer rms fit to radiosondes despite a larger bias.

6. Combined impact of MOPS cloud and screen temperature data

6.1 on screen temperatures

Further experiments were run on each trial case where MOPS, screen temperature and 10m wind data over land were not assimilated. We shall refer to these as the NMM-MOPS/$T_{1.5}$/V_{10} runs. The overall results in Figure 6 show a worthwhile benefit from both cloud and screen temperature data on screen temperature prediction, certainly to t+9 and marginally in t+12-t+18 (synop wind data were found in earlier tests to have little

impact on screen temperature prediction). Slightly more of the temperature improvement comes from the temperature data than from MOPS data.

If the anticyclonic cases are picked out (Figure 19), the benefit of the data is seen at its greatest - it is still noticeable at t+18-t+24 on days with extreme temperatures (1/9/91 and 11/12/91).

6.2 on screen level relative humidity

The overall NMM performance matches that of the OMM for DT 0z cases and betters it in an rms sense from t+3-t+18 in DT 6z cases (Figure 20). Nevertheless, there is some peculiar behaviour in the mean error for 0z cases (Figure 21), namely a large and decaying positive bias in the first 6 hours of the forecast, although this is absent in the NMM-MOPS results. A decaying cold temperature bias (Figure 7) could explain a decreasing positive relative humidity bias, but this alone does not account for the difference made by MOPS.

The early humidity bias is instead largely due to an error in the MOPS analysis of level 1 cloud cover which was discovered after the operational trial (the error was corrected operationally on 16/2/93). After the horizontal spreading of cloud data in the MOPS analysis, cloud covers of less than 1 okta are reset to zero to avoid unrealistic spreading of cloud into cloud free areas, but this procedure was not done for level 1. As a result, points with very small cloud cover were assigned a relative humidity of 92·5% (the threshold for cloud formation) in the MOPS acobs file. These large 'observed' humidities are consistent with the moist bias at the end of the assimilation period, which decays as the model recovers from the erroneous forcing. Cases with DT 0z were rerun with the error corrected and this gave significantly better verification (Figure 22), with very little bias between t+0-t+9.

6.3 on fog

In the 4/12/91 stratocumulus case, MOPS led to prediction of too much fog in cloud free areas, a problem mainly due to the error discussed above (Figure 23). The run with corrected MOPS has much less fog.

In the freezing fog case DT 6z 14/12/91, intervention in the MOPS analysis was carried out to enforce full cloud cover where sky obscured or near full cover was reported. Cloud base heights were set to zero and cloud top heights to 300 feet in foggy areas. The NMM t+3 visibility prediction agrees reasonably with observations over southern England (Figure 24). A study of the NMM-MOPS and NMM-MOPS/$T_{1.5}$/V_{10} frames reveals, however, that most of the impact comes from screen temperature data rather than MOPS. The NMM-MOPS run also retains some fog through the day to 18z, whereas the NMM-MOPS/$T_{1.5}$/V_{10} run loses all fog in southern England after 9z.

7. Impact of surface data on pressure pattern

In general there is little impact of the NMM or its extra data on the surface pressure pattern relative to the LAM. An exceptional case (not formally included in the operational trial) was that of the small scale low

first analysed operationally over Ireland at 12z, 12/11/91. Analyses and t+6 forecasts are shown in Figures 25 and 26. From the two mesoscale runs shown, it is evident that the extra synop wind data help increase the circulation around the low. The main impact on this forecast comes from model resolution - the NMM is significantly better than the LAM. OMM runs are not available for direct comparison with these unified model runs.

Synop wind data (along with screen temperature data) are found to have very little impact on objective verification of the 10m wind field, the margin of improvement in rms wind speed is at best 0·4 knots at t+3 and 0·1 knots at t+6.

APPENDIX A - Basic decription of the new operational mesoscale model

Domain and resolution

Figure A1 shows the NMM domain and grid points within a subset of those for the LAM. The NMM gridlength is 0·15° (about 16·7km) and the domain is 92x92 points. The NMM orographic height (Figure A2) is derived from data at a resolution of 0·083°. The timestep is 90 seconds.

There are 30 vertical levels, with those above about 8km matching levels in the LAM and global models. The lowest 10 hybrid levels (Figure A3) are sigma levels, while the top 3 are pressure levels. The relative heights in metres of LAM and NMM levels are given in Figure A4. They share the same bottom level at 25m, but the NMM resolution is significantly finer in the boundary layer. The boundary layer scheme operates on the bottom 13 NMM levels.

Surface characteristics

Ancillary fields are derived from the 1° unified model datasets. The roughness length dataset is tailored to the NMM, accounting not only for vegetative effects as in the LAM but also the influence of mountains, lakes, grass, trees and buildings. Roughness lengths for heat and moisture are taken to be 1/5th of those for momentum.

Physical parametrisations

The NMM physics package includes several ingredients not present in the current operational version of the LAM, although they are likely to be incorporated into the LAM in spring 1993. The NMM has a convective downdraught scheme, a new formula for the evaporation of rain consistent with the convection scheme and a 'rapidly mixing' boundary layer scheme. The radiation scheme is called hourly instead of 3-hourly as in the LAM and the NMM short-wave scheme takes account of the updated solar angle every timestep. Gravity wave drag is switched off in the NMM.

Diffusion

The NMM currently has a ∇^2 horizontal scheme for all variables, with a coefficient of $K=4\times10^4$ m^2s^{-1}. Divergence damping in the assimilation has a coefficient $K_D=10^5$ m^2s^{-1}. Vertical diffusion is switched off.

APPENDIX B - NMM trial cases

		interest
1.	DT 0z, 6/7/91	thunderstorms
2.	DT 0z, 23/8/91	spiral vortex with precipitation bands
3.	DT 0z, 1/9/91	hot day
4.	DT 0z, 8/9/91	sea breeze development
5.	DT 6z, 8/11/91	cold unstable northwesterly airstream
6.	DT 0z, 4/12/91	stratocumulus
7.	DT 6z, 11/12/91	cold night
8.	DT 6z, 14/12/91	freezing fog
9.	DT 6z, 17/2/92	snow

ACKNOWLEDGEMENTS

We would like to thank Sue Ballard, Richard Barnes, Simon Jackson, Bob Robinson and Steve Woltering in the modelling section of the mesoscale group for their role in setting up and running the NMM trial experiments, for their analyses and interpretation of the results and for suggesting aspects of the assimilation scheme worthy of further investigation.

REFERENCES

Ballard, S.P. and Robinson, R., 1993, 'Development and performance of the new mesoscale model.' Forecasting Research Tech. Rep. No 40.

Cullen, M.J.P., 1991, 'The unified forecast/climate model.' Short-range Forecasting Research Sci. Pap. No 1.

Golding, B., 1990, 'The Meteorological Office mesoscale model.' Meteorol. Mag., 119, 81-96.

Lorenc, A.C., Bell, R.S. and Macpherson, B., 1991, 'The Meteorological Office analysis correction data assimilation scheme.' Q.J.R. Meteorol. Soc., 117, 59-89.

Wright, B.J., 1993, 'The Moisture Observation Pre-processing System.' Forecasting Research Tech. Rep. No 38.

Wright, B.J., and Golding, B., 1990, 'The Interactive Mesoscale Initialization.' Meteorol. Mag., 119, 234-244.

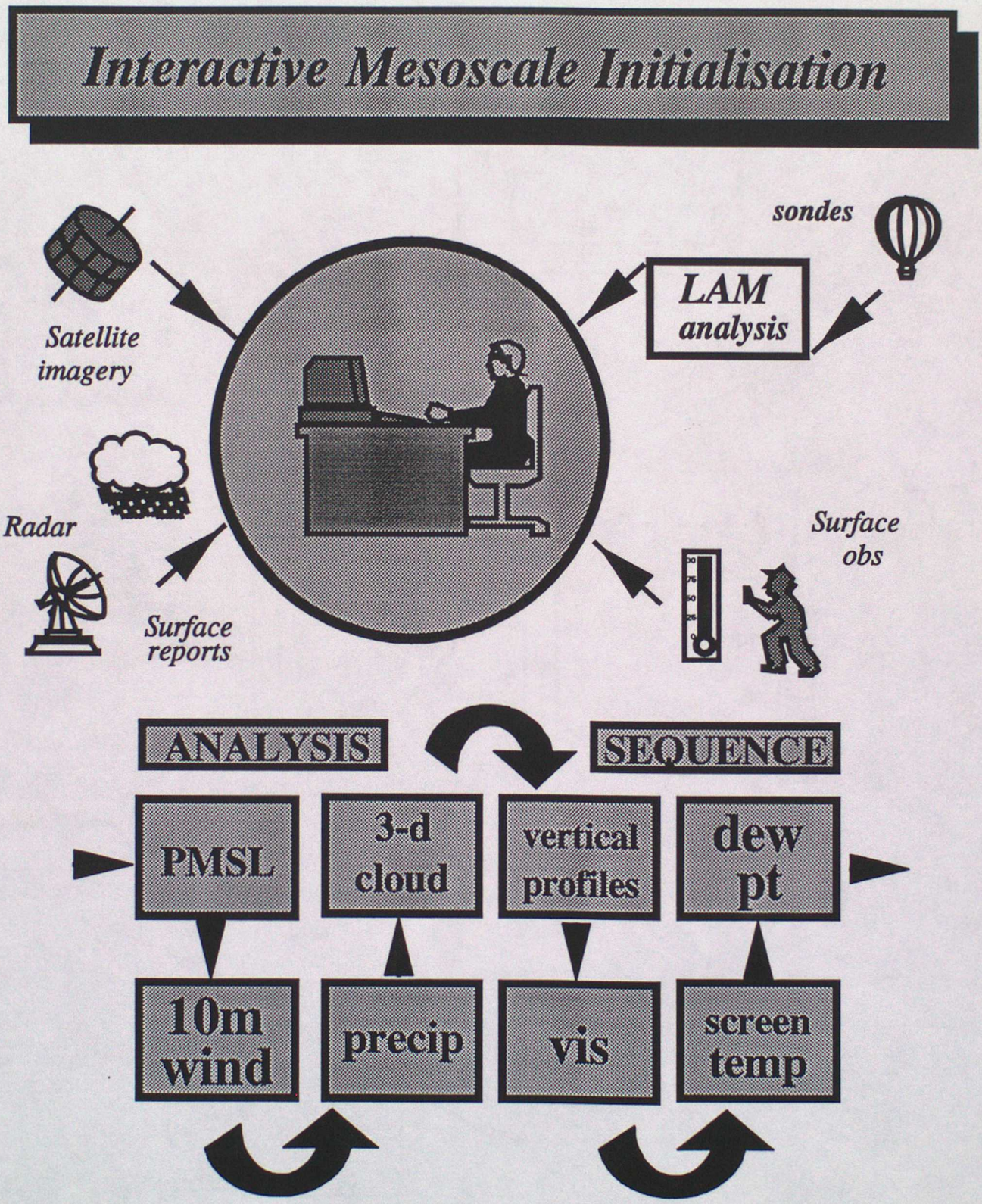

FIGURE 1: Initialisation scheme for the old mesoscale model

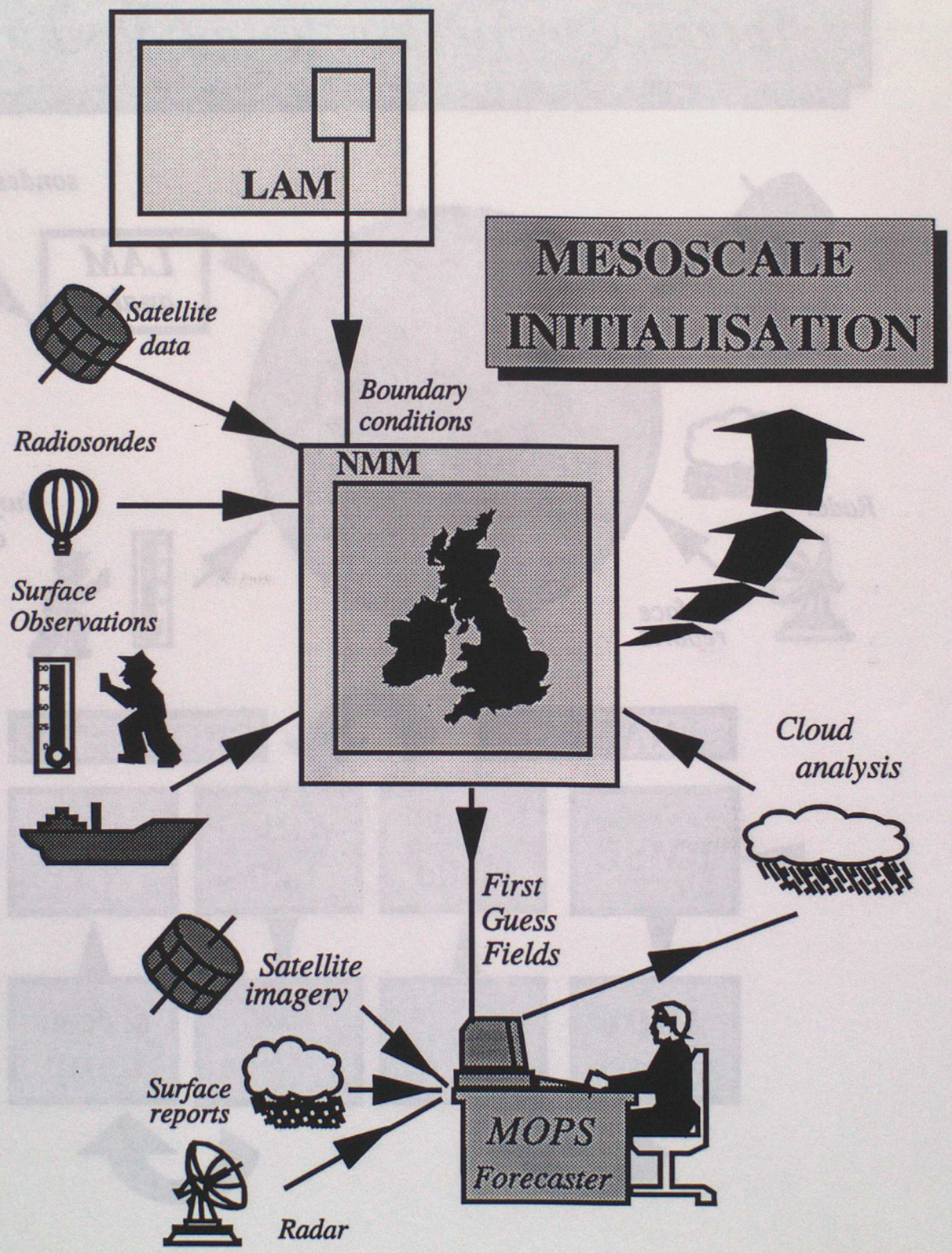

FIGURE 2: Assimilation scheme for the new mesoscale model

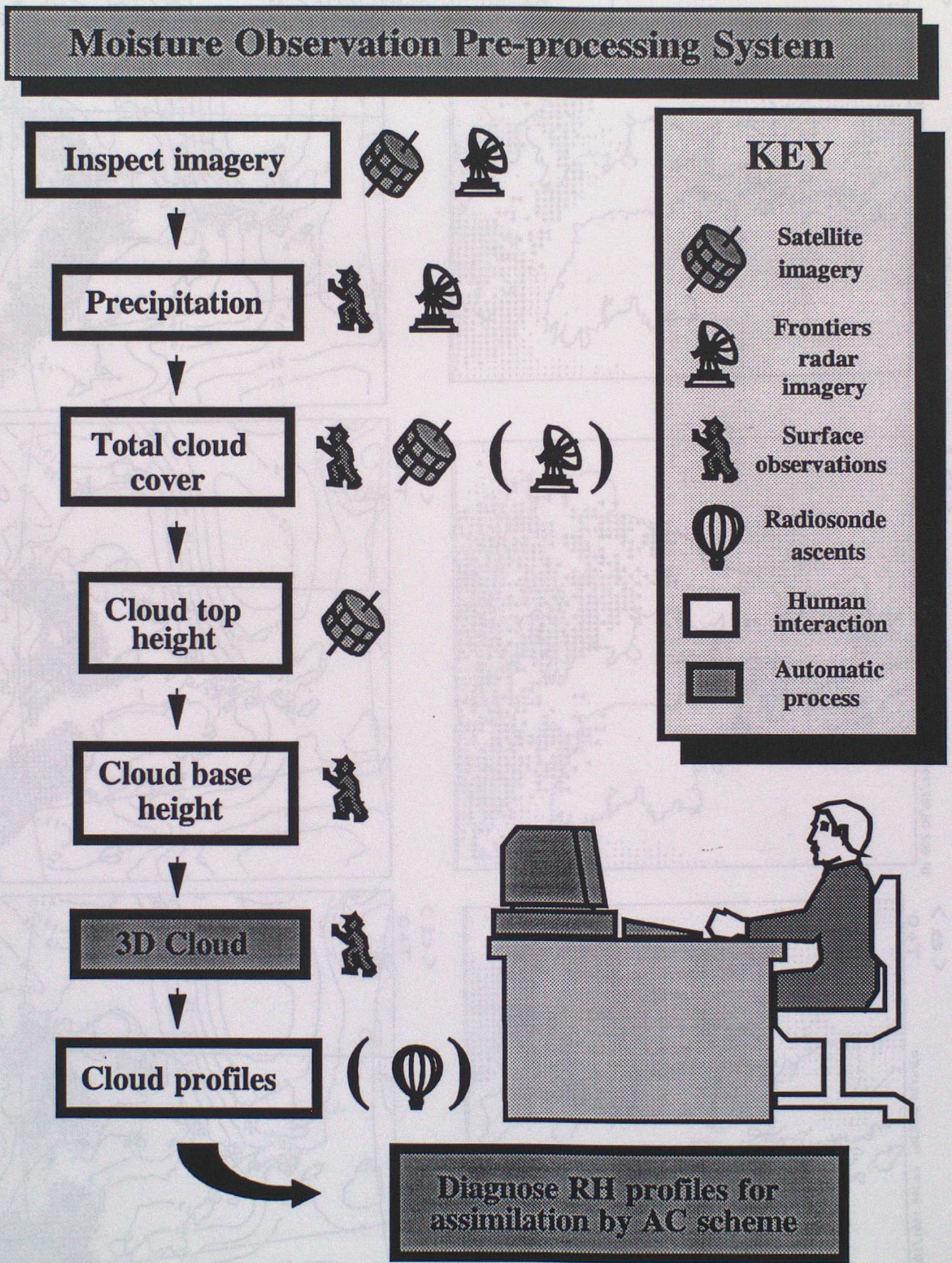

FIGURE 3: MOPS for the new mesoscale model

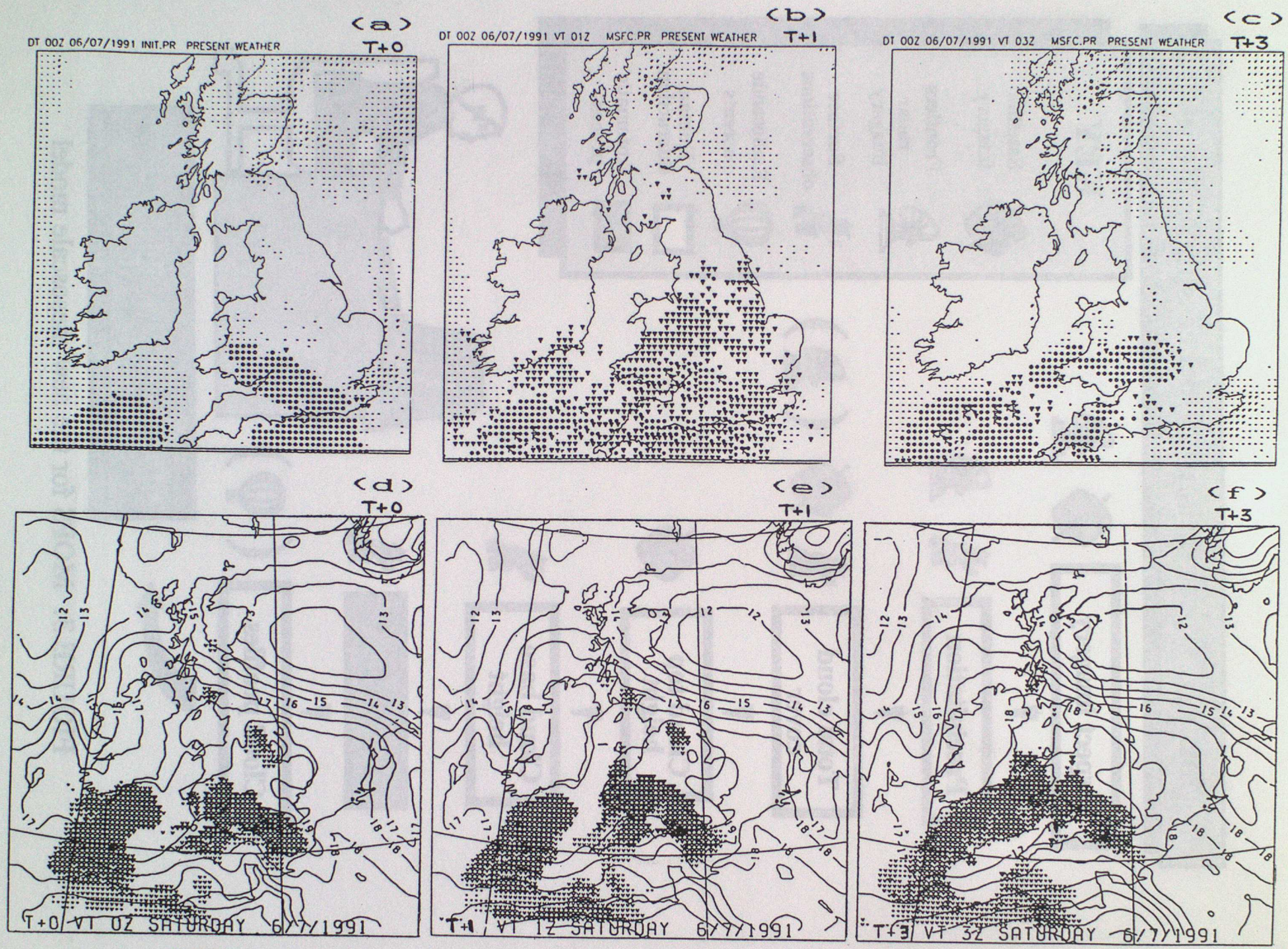

FIGURE 4: Top (a,b,c) - OMM present weather at t+0, t+1, t+3 from DT 0z, 6/7/91
Bottom (d,e,f) - NMM precipitation (and 850mb θ_w) for same times.

FIGURE 5(a)

Mean cloud cover errors
average over 5 DT 0Z cases

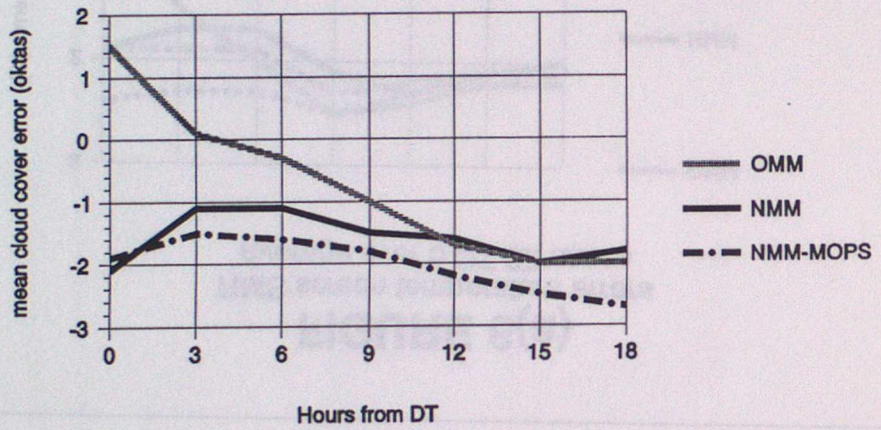

FIGURE 5(b)

Mean cloud cover errors
average over 4 DT 6Z cases

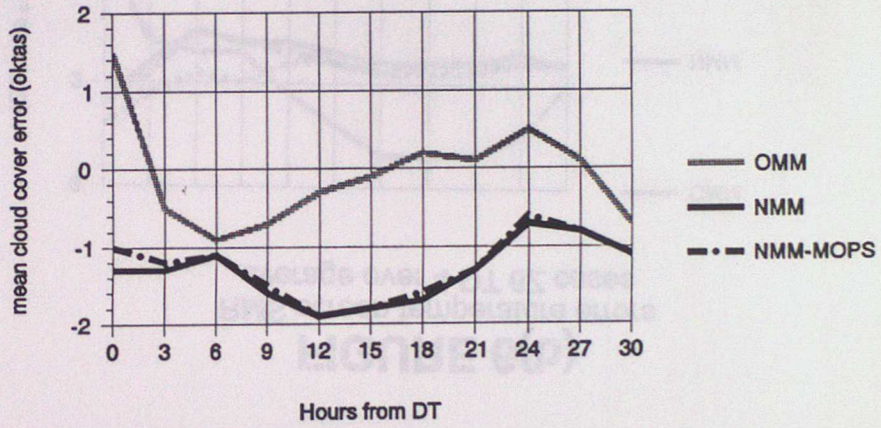

FIGURE 6(a)

RMS screen temperature errors
average over 5 DT 0Z cases

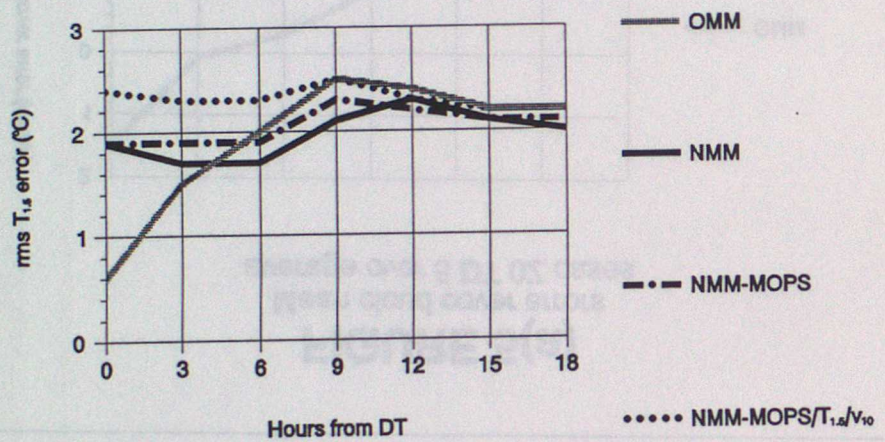

FIGURE 6(b)

RMS screen temperature errors
average over 4 DT 6Z cases

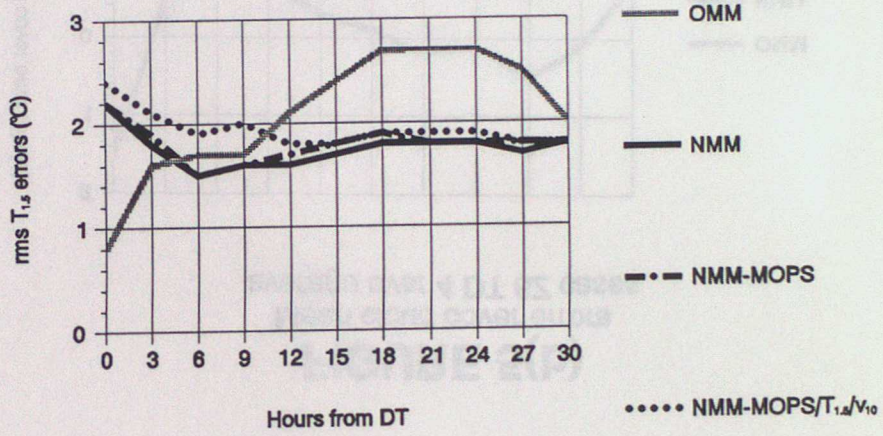

FIGURE 7(a)

Mean screen temperature error
average over 5 DT 0Z cases

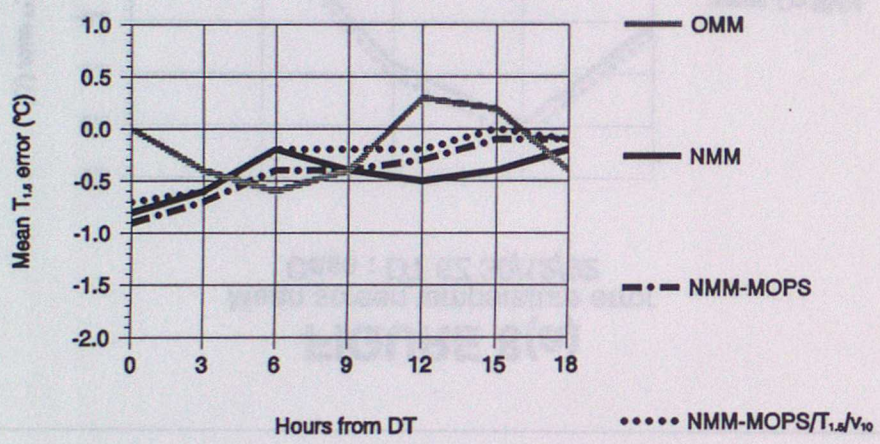

FIGURE 7(b)

Mean screen temperature error
average over 4 DT 6Z cases

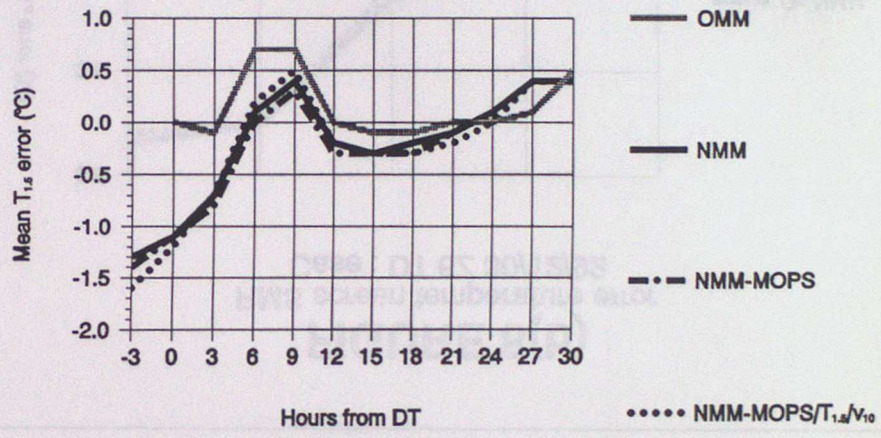

FIGURE 8(a)

Mean screen temperature error
Case : DT 6Z 30/12/92

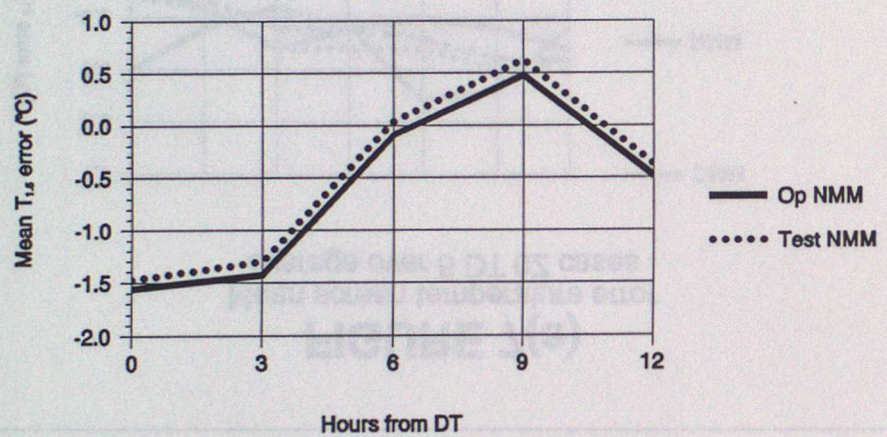

FIGURE 8(b)

RMS screen temperature error
Case : DT 6Z 30/12/92

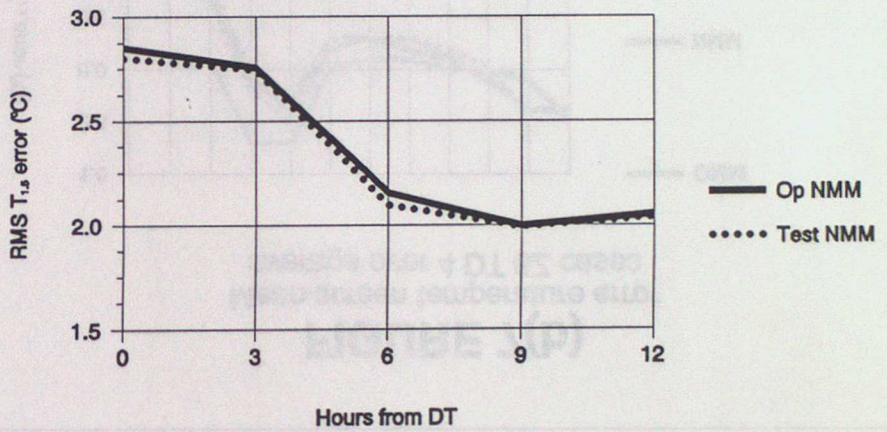

FIGURE 9(a)
DT 0Z 1/9/1991

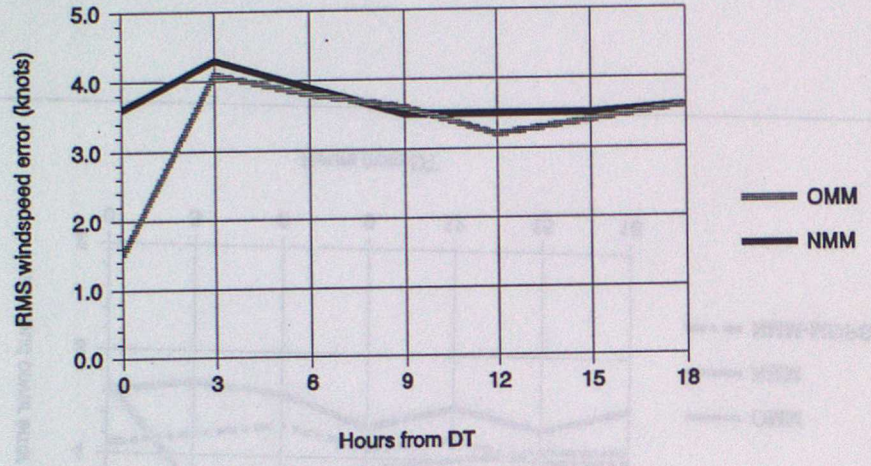

FIGURE 9(b)
DT 0Z 4/12/1991

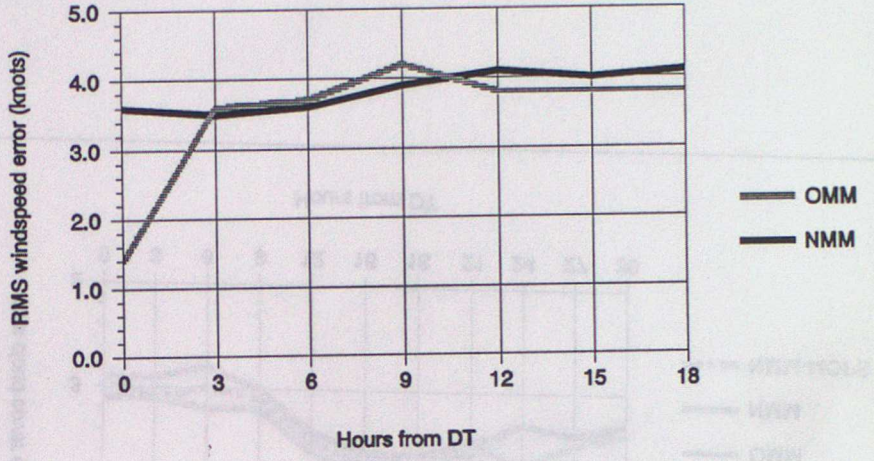

FIGURE 9(c)
DT 0Z 8/9/1991

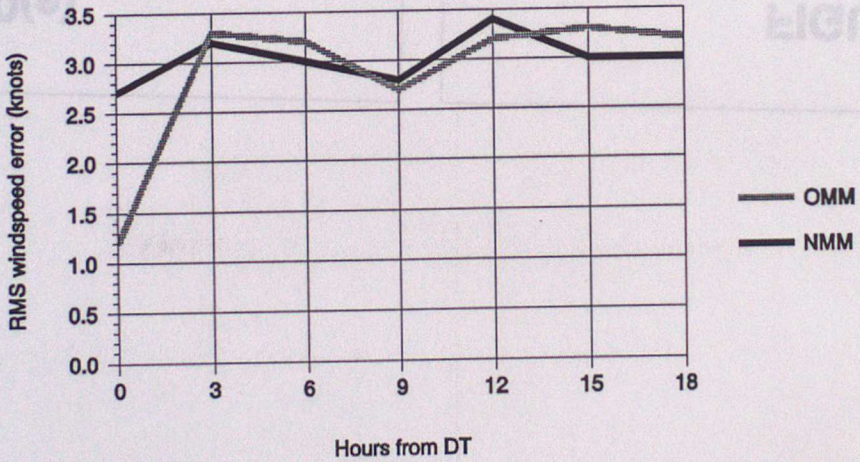

FIGURE 10(a)

RMS cloud cover errors
average over 5 DT 0Z cases

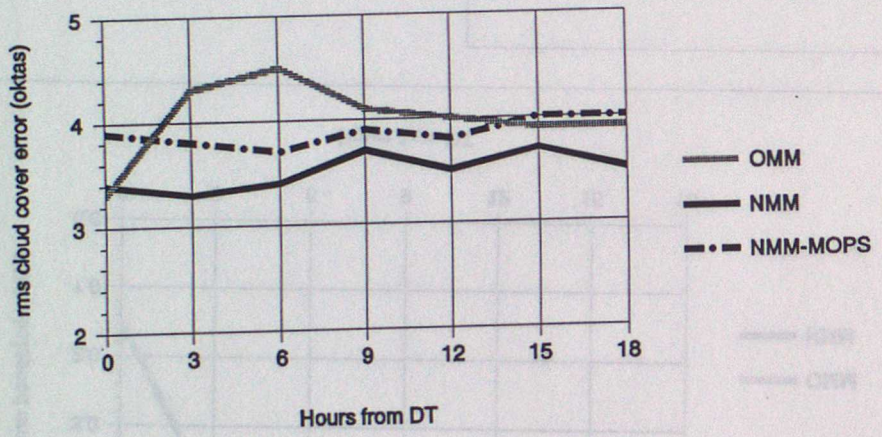

FIGURE 10(b)

RMS cloud cover errors
average over 4 DT 6Z cases

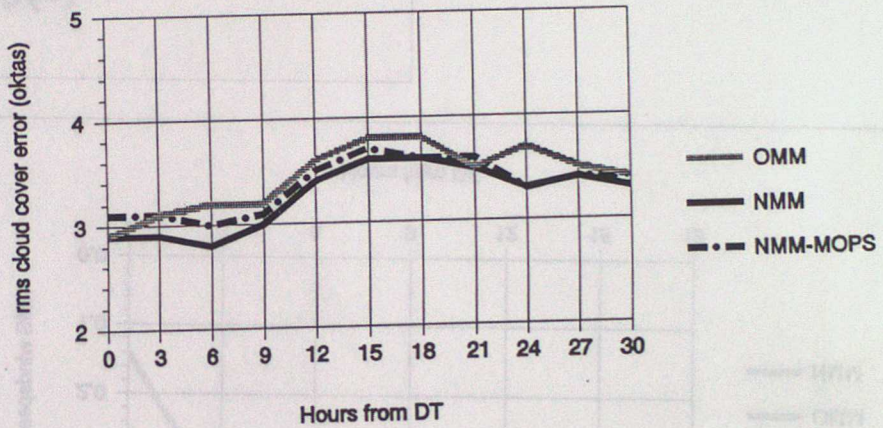

FIGURE 11

Cloud base height verification

percentage correct in 3 categories : 0-1000 ft, 1000-2000 ft, 2000-5000 ft

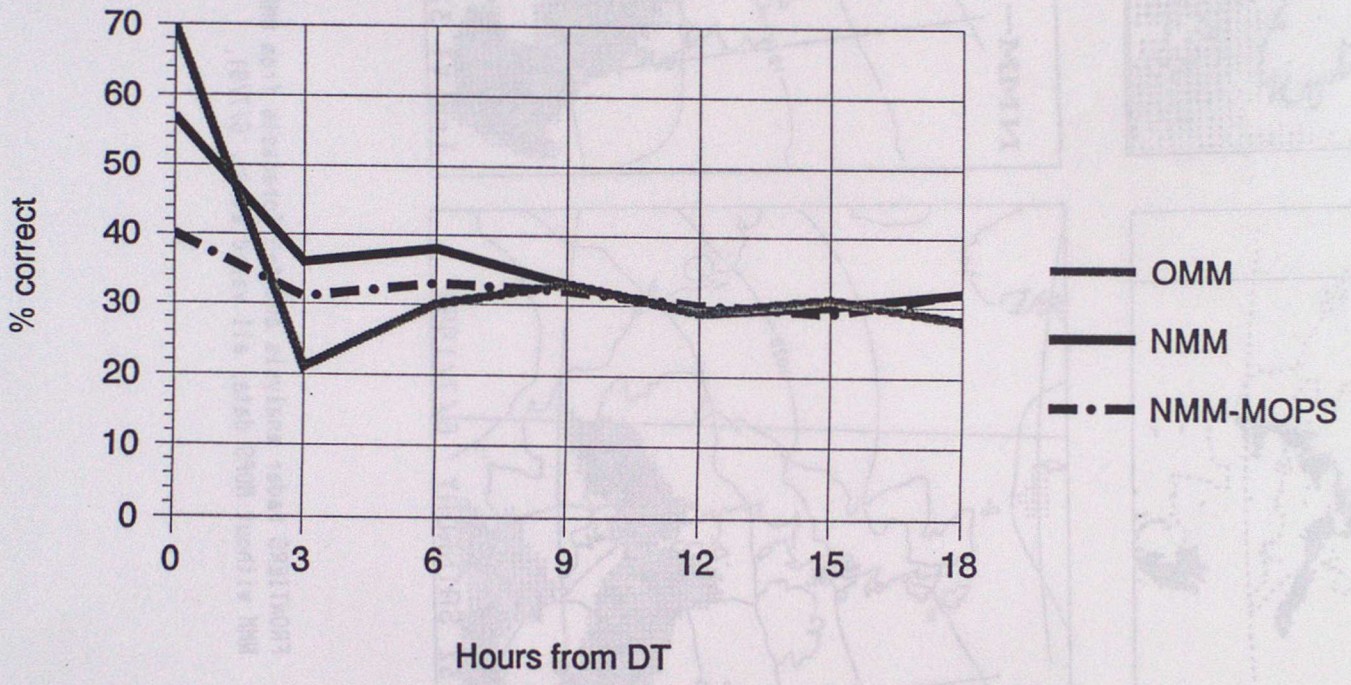

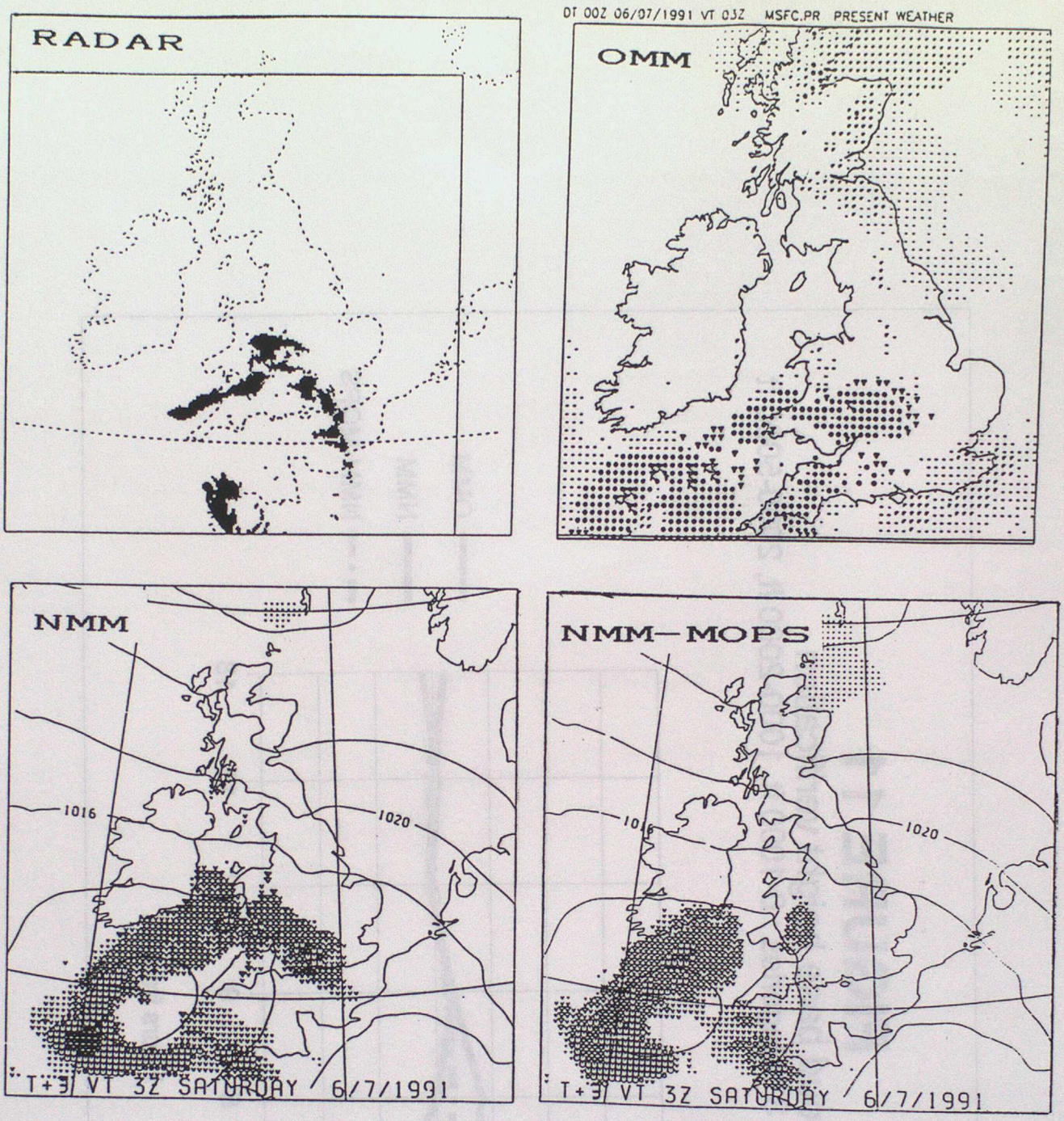

FIGURE 12: FRONTIERS radar analysis and t+3 forecasts from OMM, NMM and NMM without MOPS data, all valid at 3z, 6/7/91.

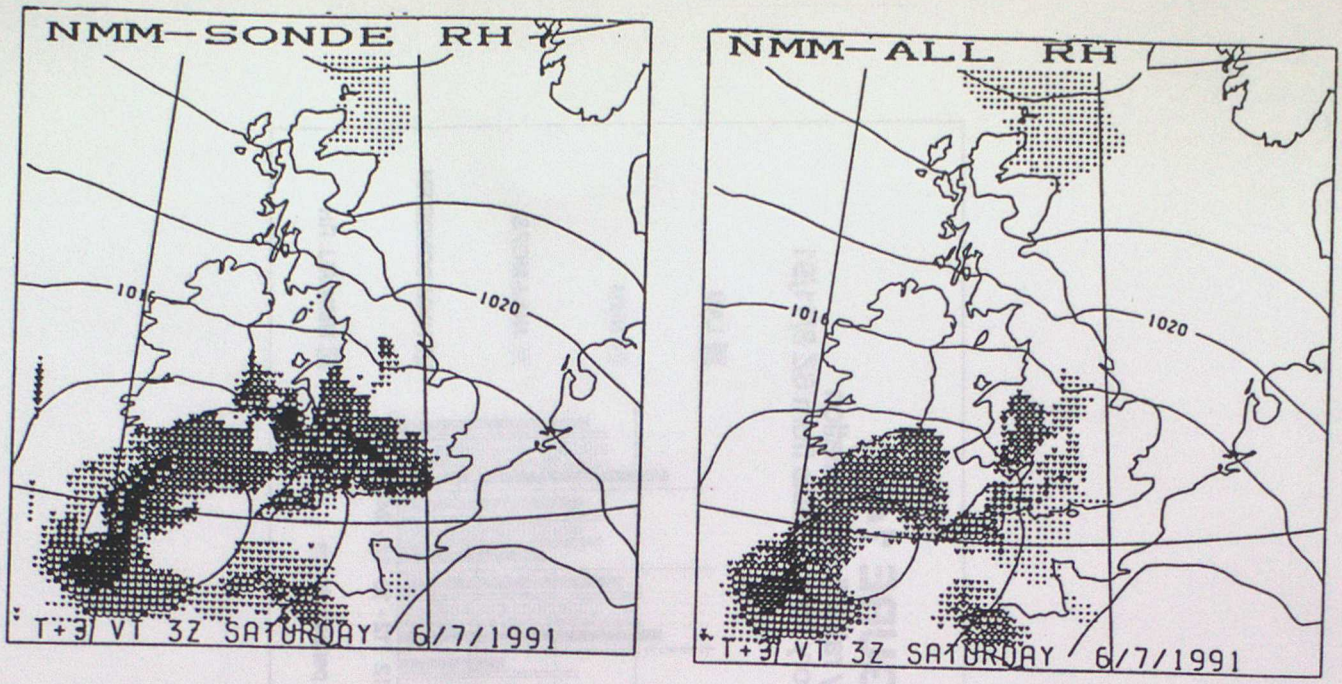

FIGURE 13: t+3 forecasts from NMM without radiosonde humidity data and from NMM without any humidity data. Valid at 3z, 6/7/91 as in Figure 12.

FIGURE 14(a)

6-hourly rainfall accumulation
% in correct category for forecasts from 0Z 6/7/91

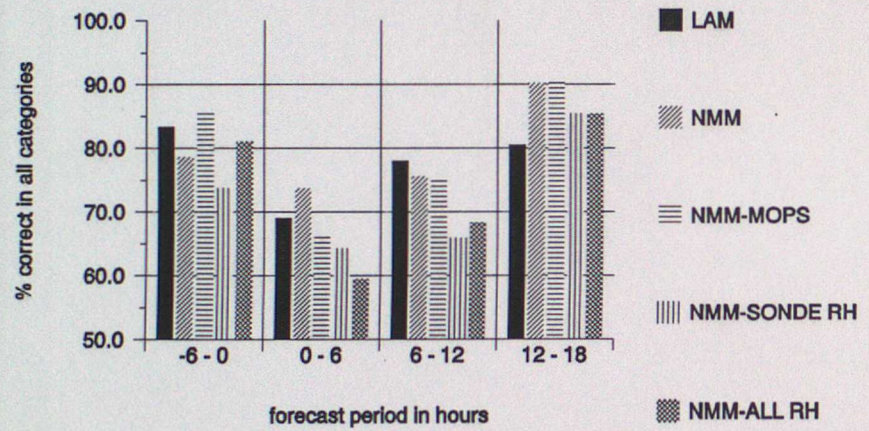

FIGURE 14(b)

6-hourly rainfall accumulation
% in correct category for forecasts from 6Z 8/11/91

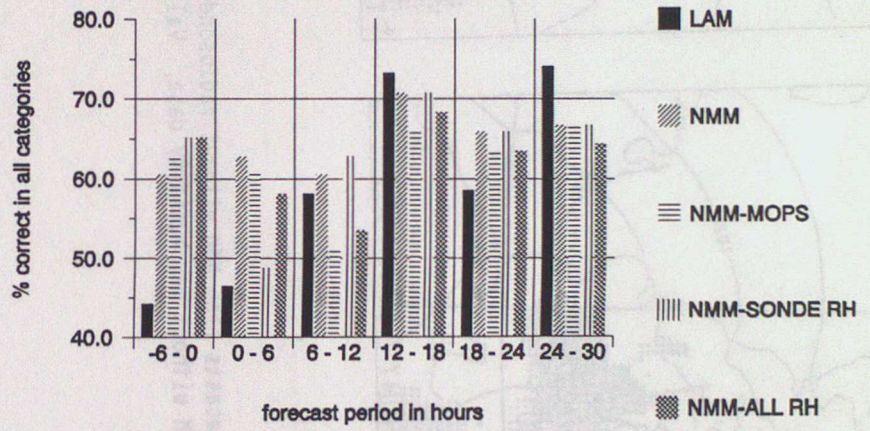

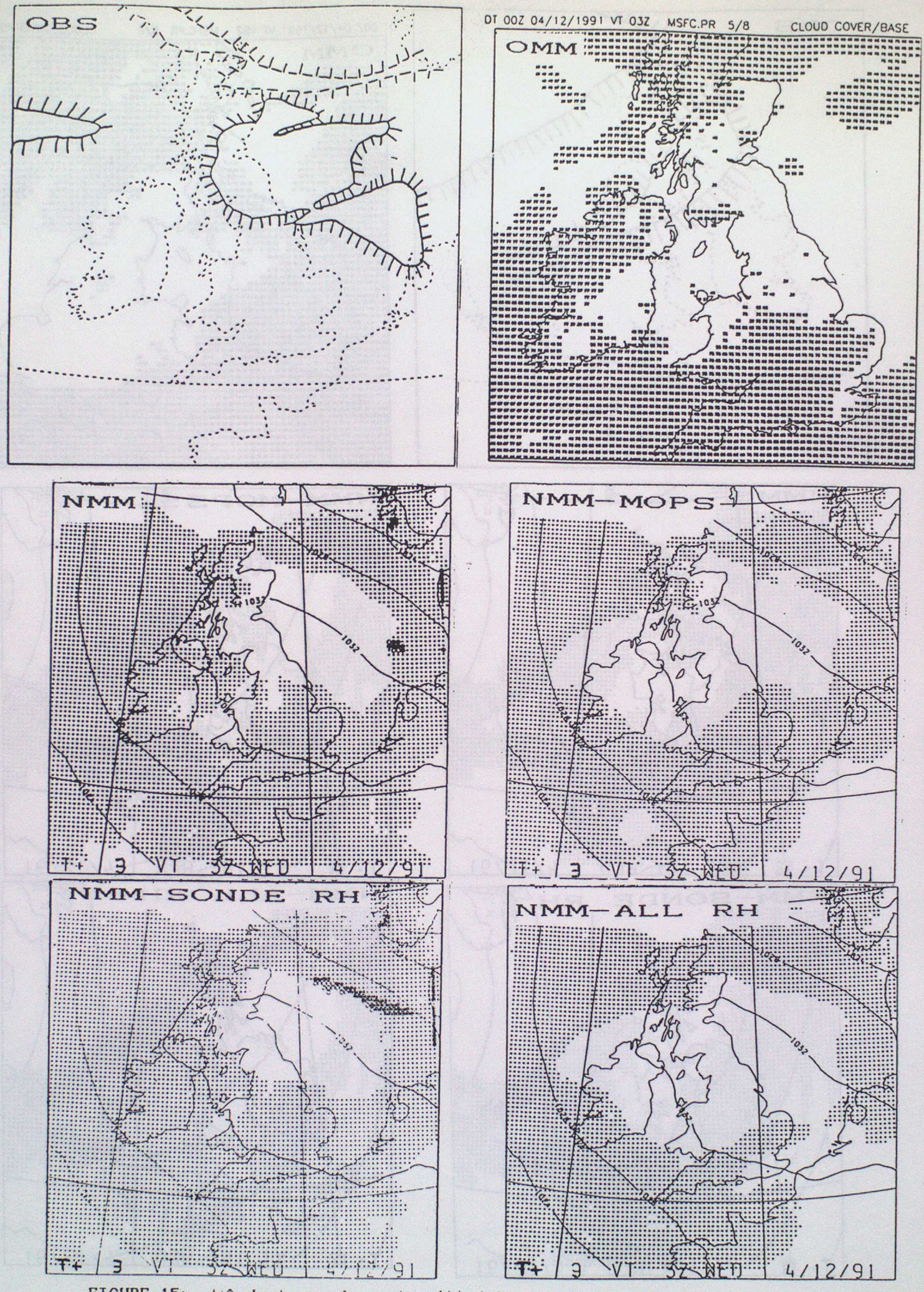

FIGURE 15: t+3 cloud cover forecasts valid at 3z, 4/12/91 and schematic verifying analysis of cloud edge from surface data and satellite imagery (labelled OBS) The OMM shows amounts of greater than 3 oktas, the NMM threshold is 4 oktas. The NMM output shows a dot for low cloud, an open circle for medium cloud and a black circle where both low and medium cloud coincide.

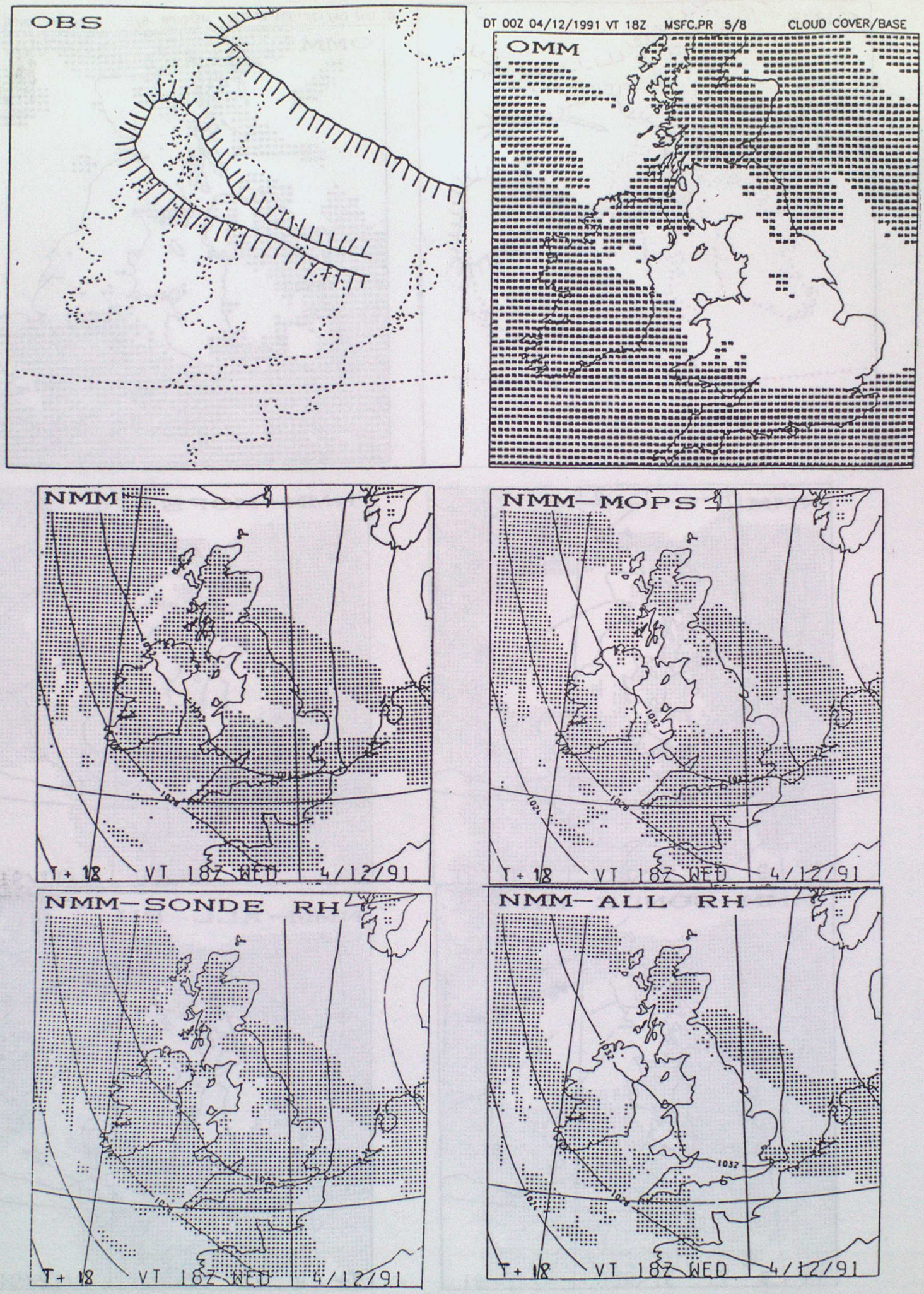

FIGURE 16: t+18 cloud cover forecasts valid at 18z, 4/12/91
Rest as in Figure 15.

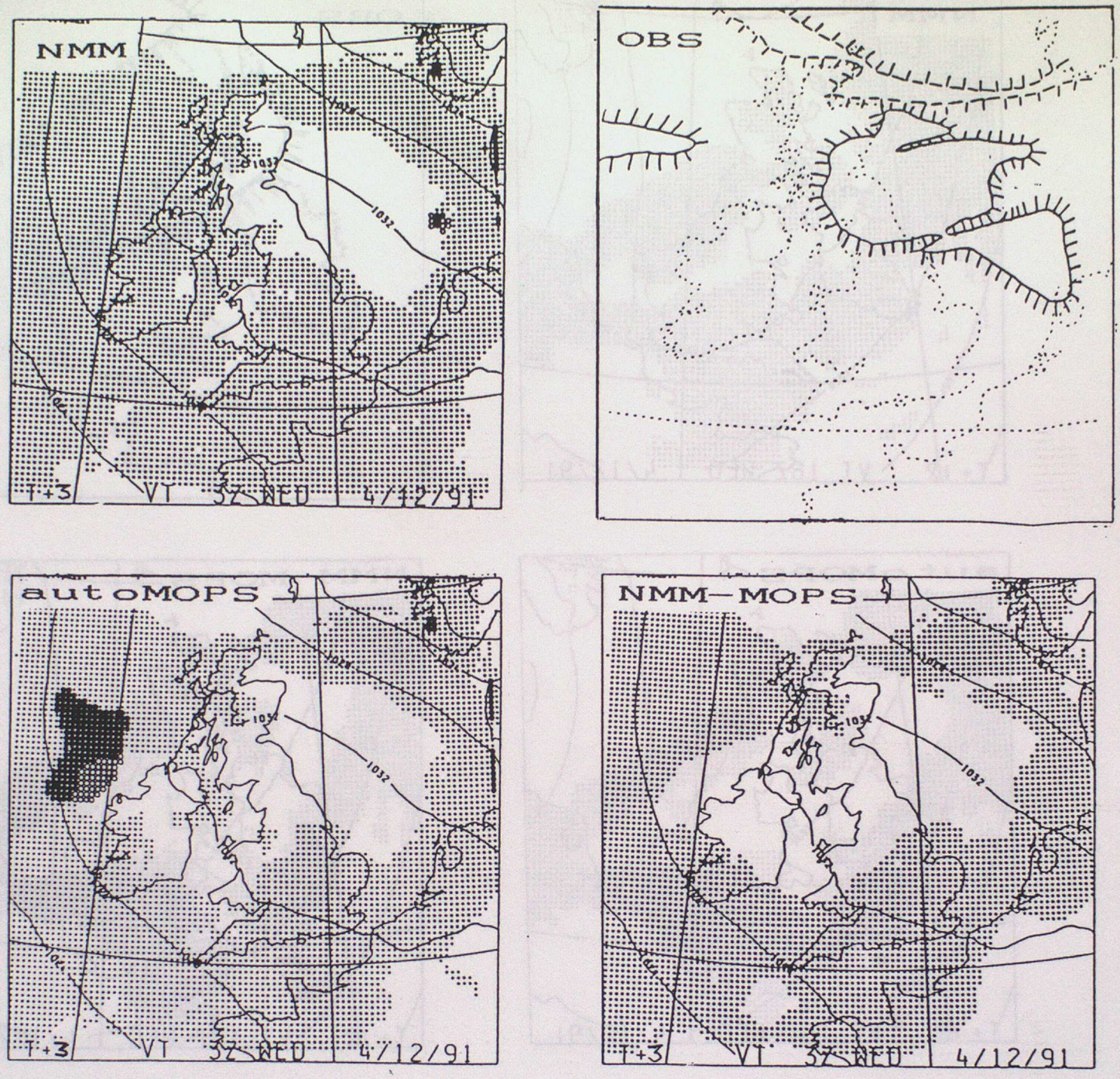

FIGURE 17(a): t+3 cloud cover forecasts as in Figure 15 but demonstrating the impact of human intervention in MOPS (as in the NMM run) relative to a run with automatic MOPS data preparation (autoMOPS run).
The NMM-MOPS and OBS frames provide references.

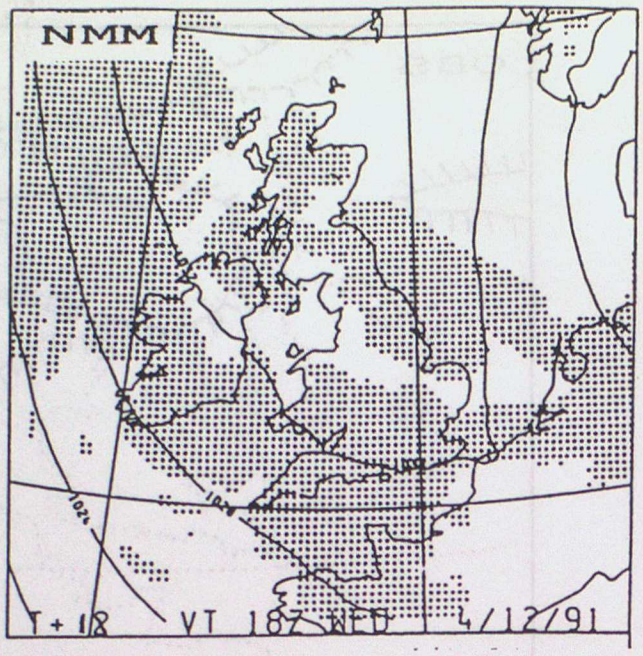

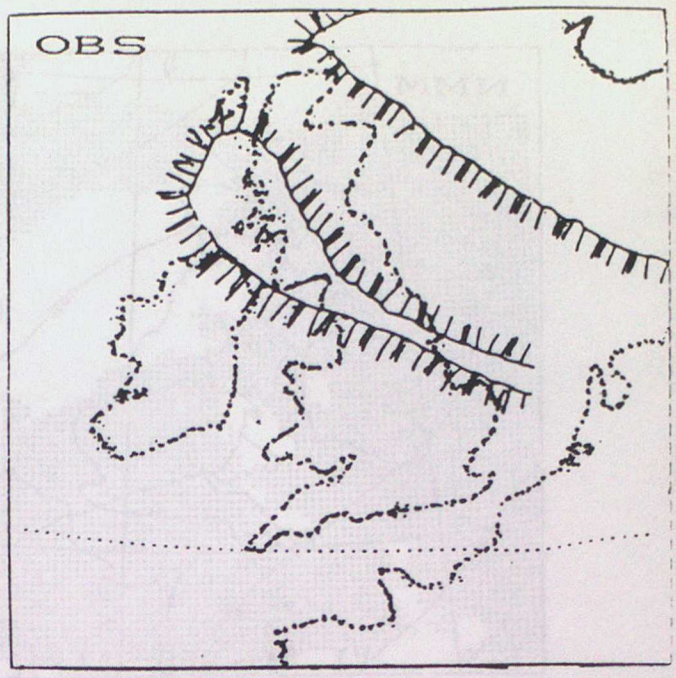

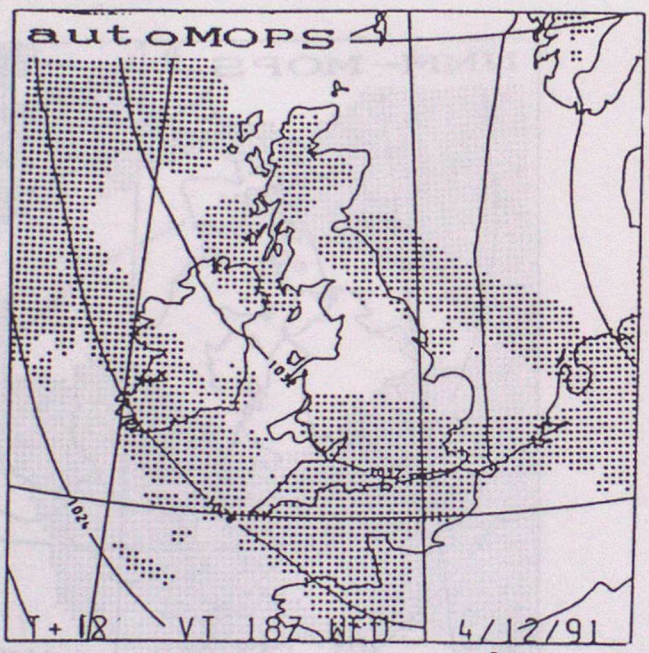

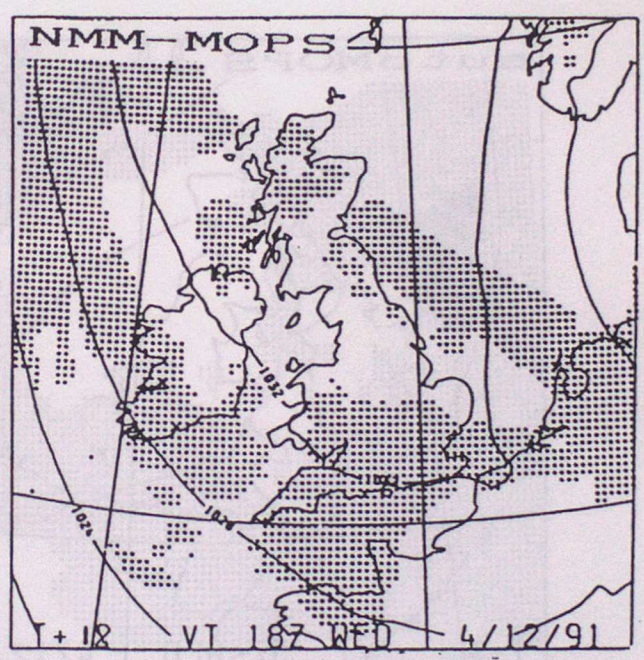

FIGURE 17(b): as in Figure 17(a) for t+18.

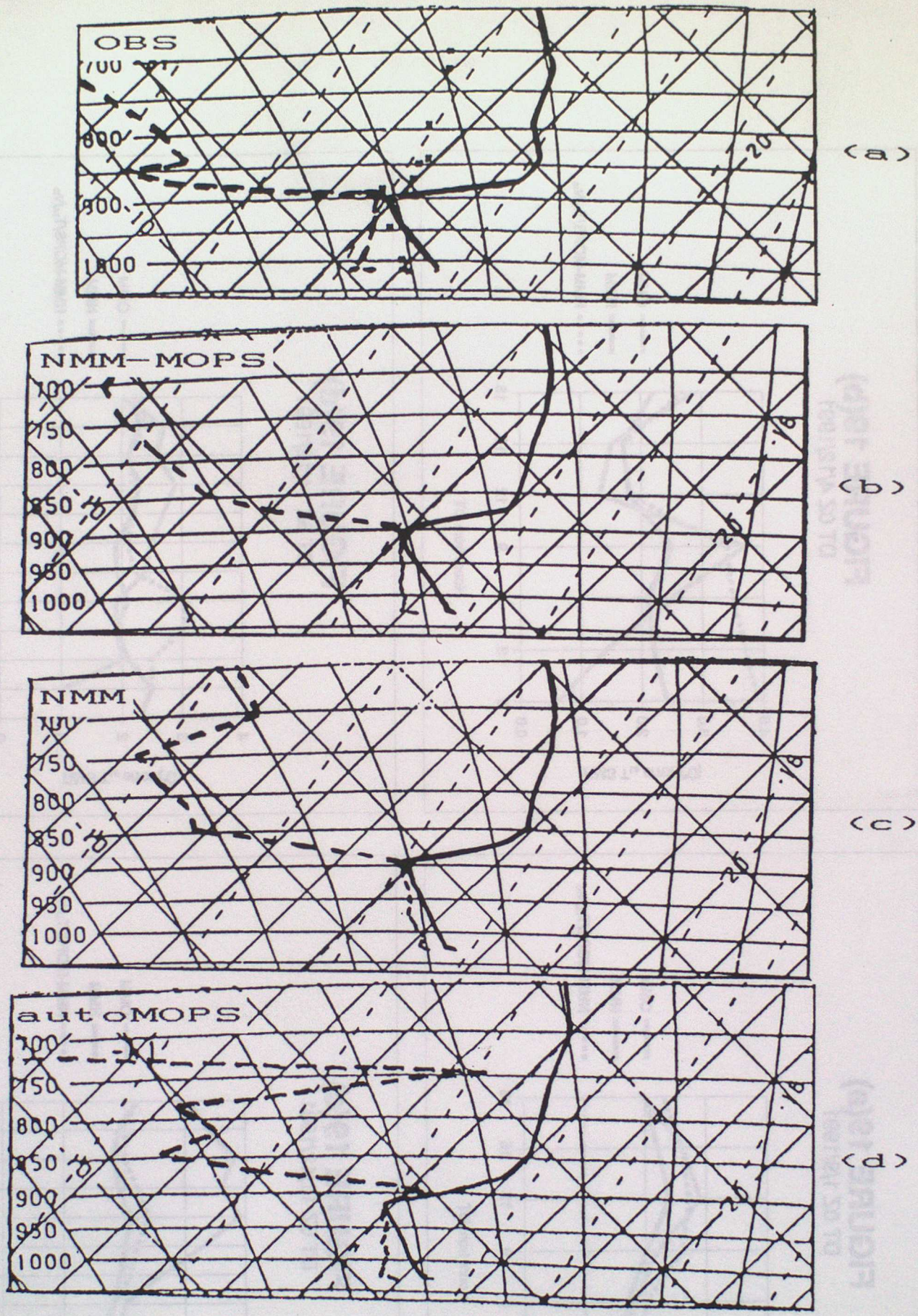

FIGURE 18: Observed and various model t+0 ascents for Camborne at 0z, 4/12/91.

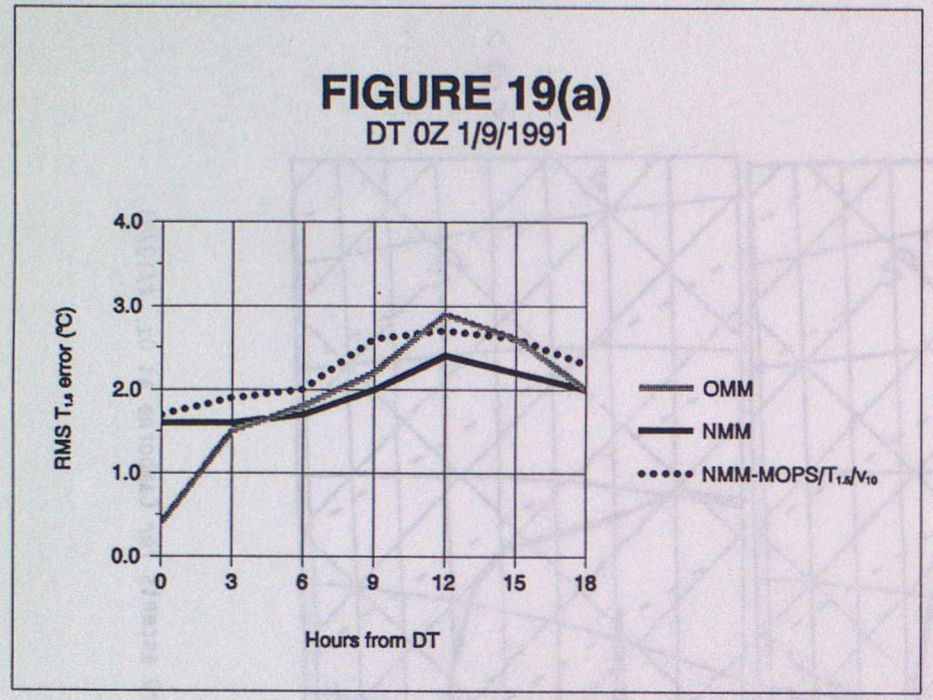

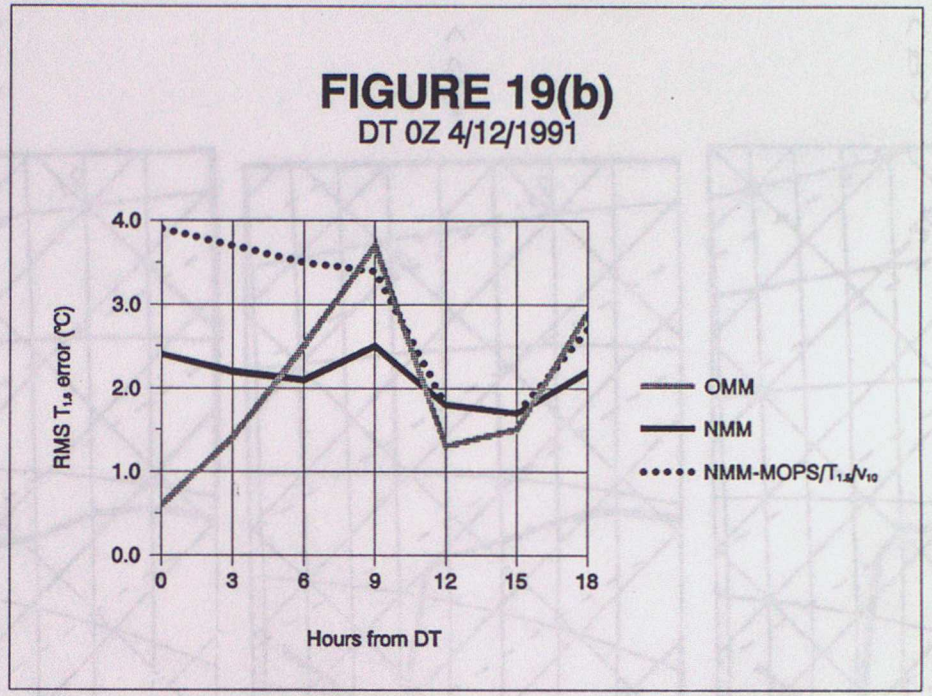

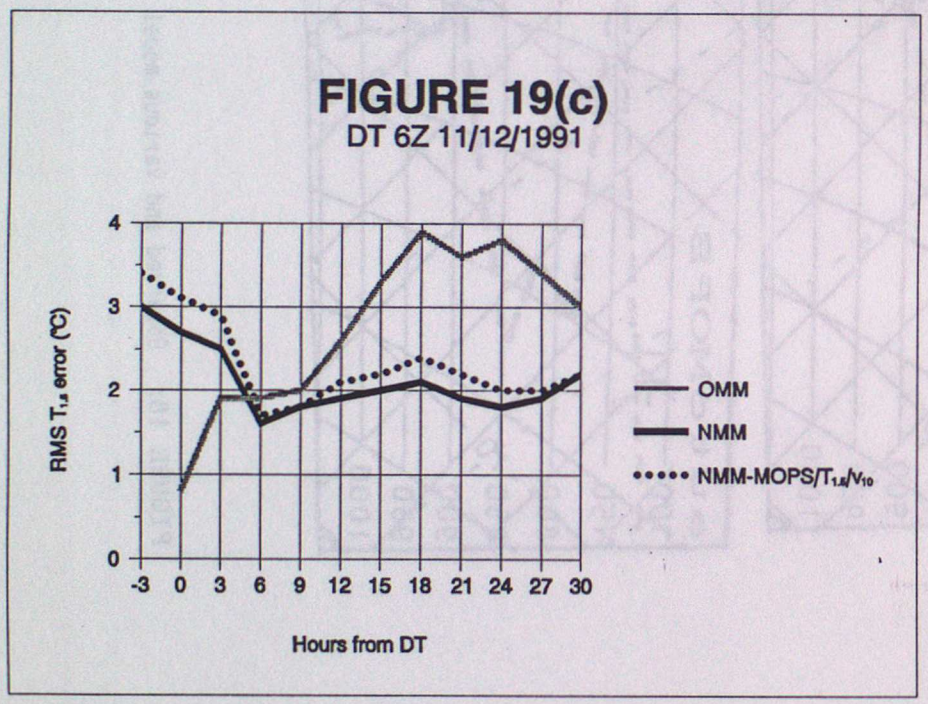

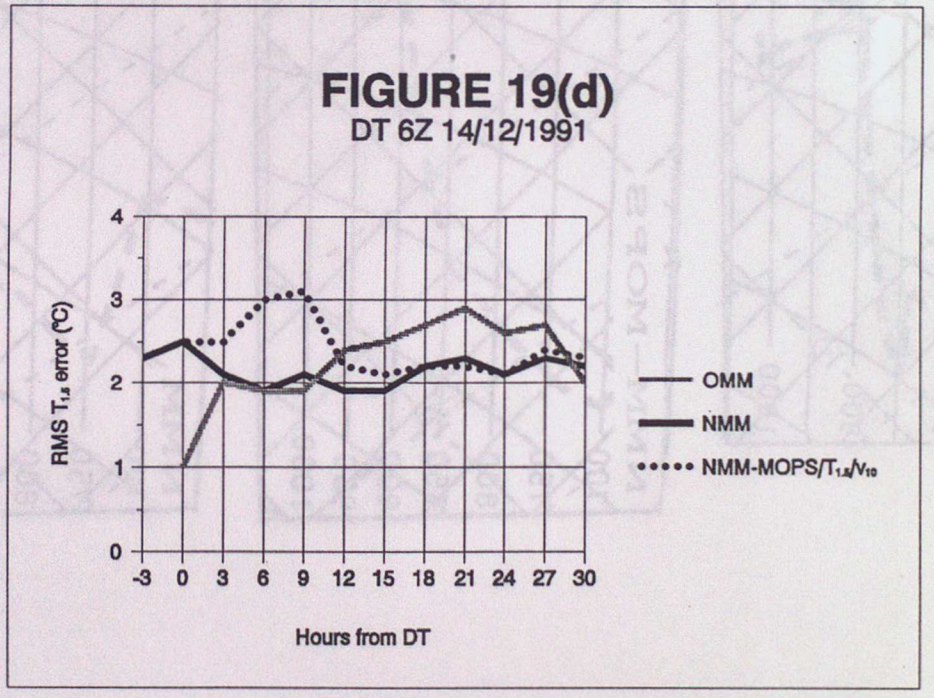

FIGURE 19: Screen temperature verification for anticyclonic cases.

FIGURE 20(a)

RMS screen RH error
average over 5 DT 0Z cases

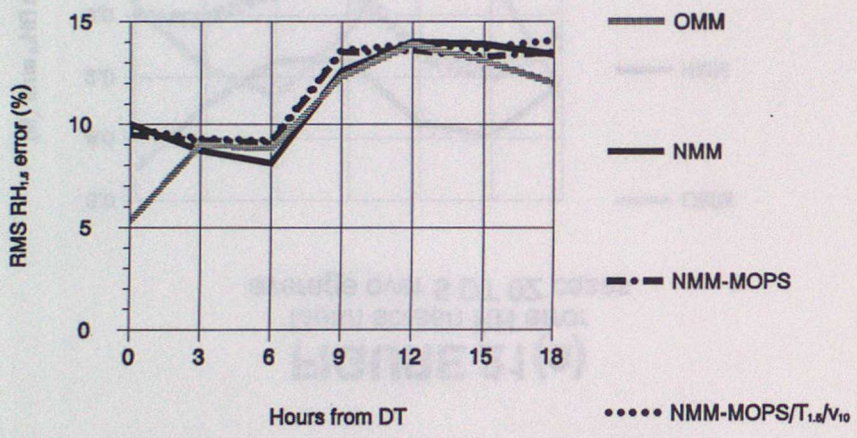

FIGURE 20(b)

RMS screen RH error
average over 4 DT 6Z cases

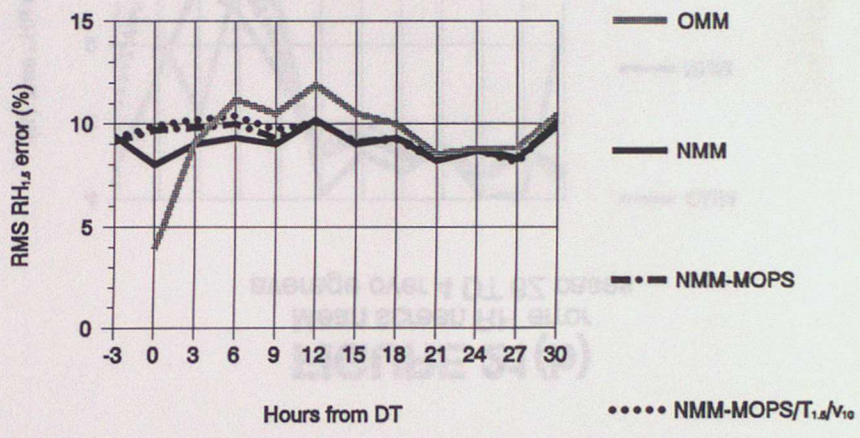

FIGURE 21(a)

Mean screen RH error
average over 5 DT 0Z cases

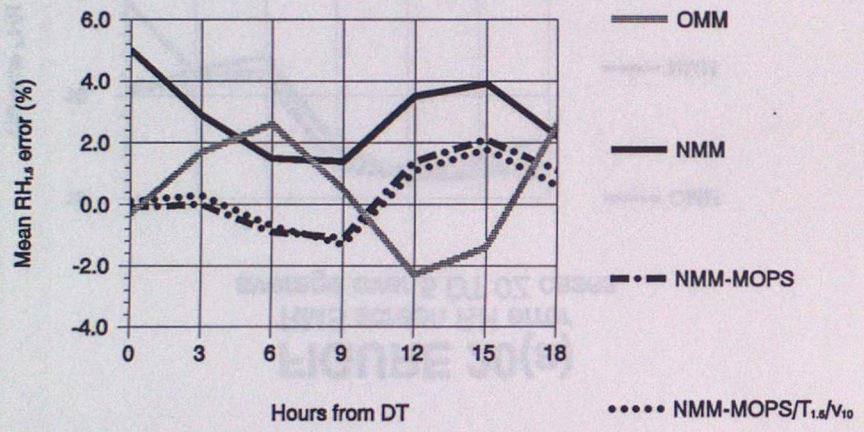

FIGURE 21(b)

Mean screen RH error
average over 4 DT 6Z cases

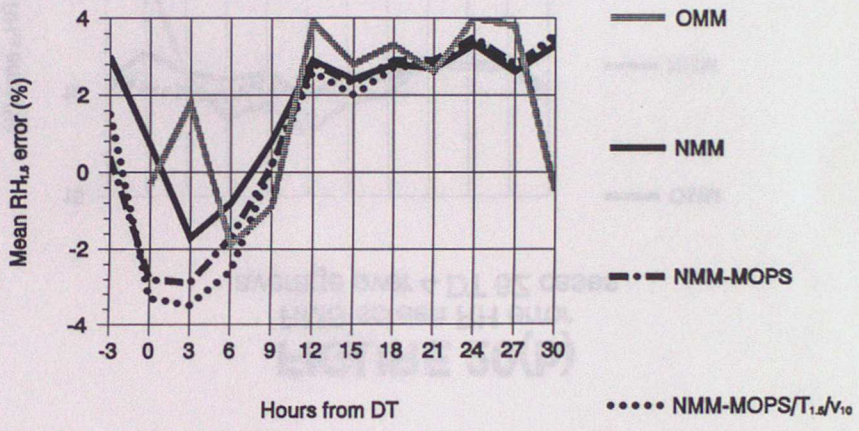

FIGURE 22(a)

Impact of MOPS correction on mean screen RH error
average over 5 DT 0Z cases

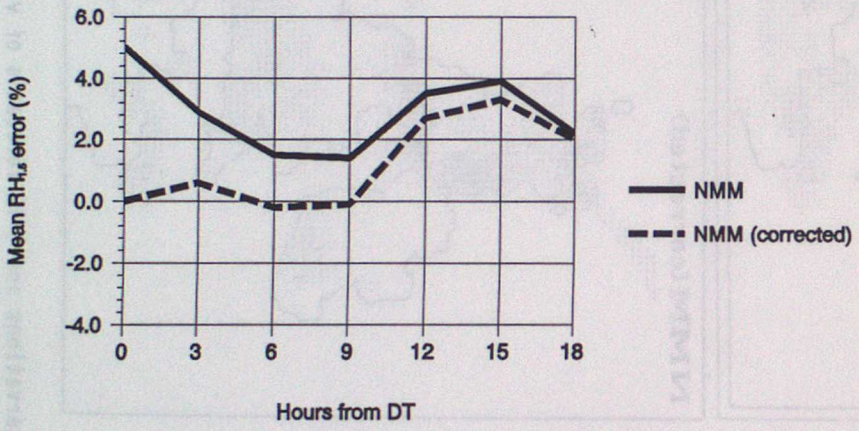

FIGURE 22(b)

Impact of MOPS correction on RMS screen RH error
average over 5 DT 0Z cases

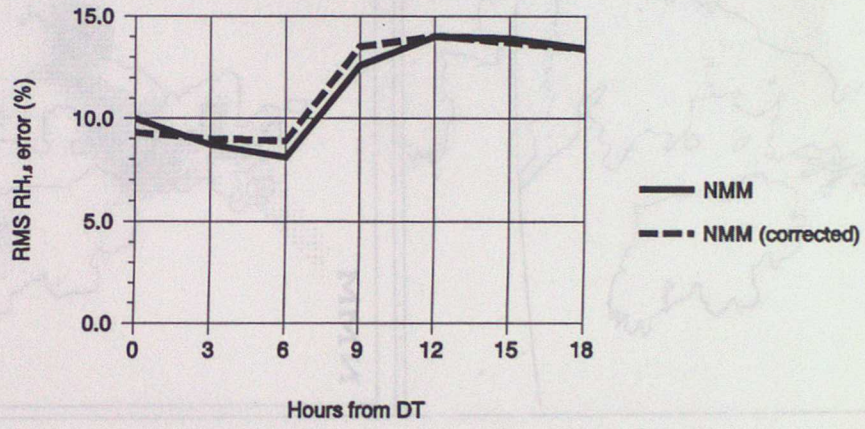

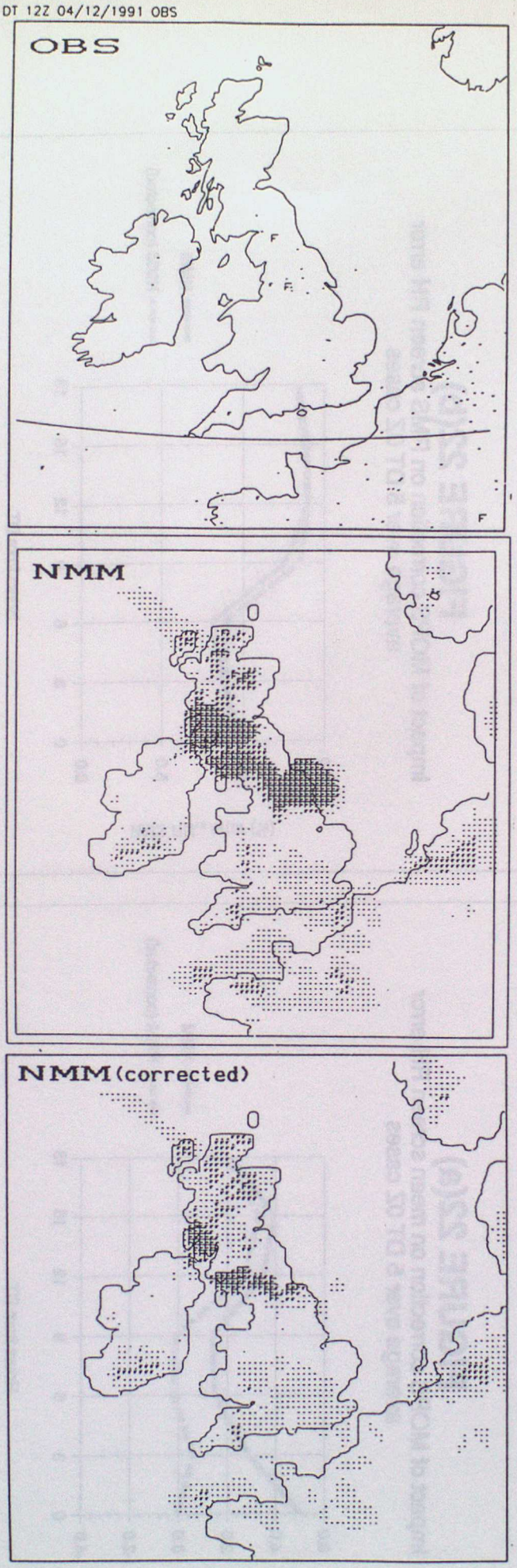

FIGURE 23: Observations and t+12 forecasts of visibility at 12z, 4/12/91. The NMM(corrected) run shows the effect of correcting an error in the preparation of MOPS data at level 1 that is present in the NMM run. Symbols denote visibility <5km (-), <1km (F), <0·2km (F)

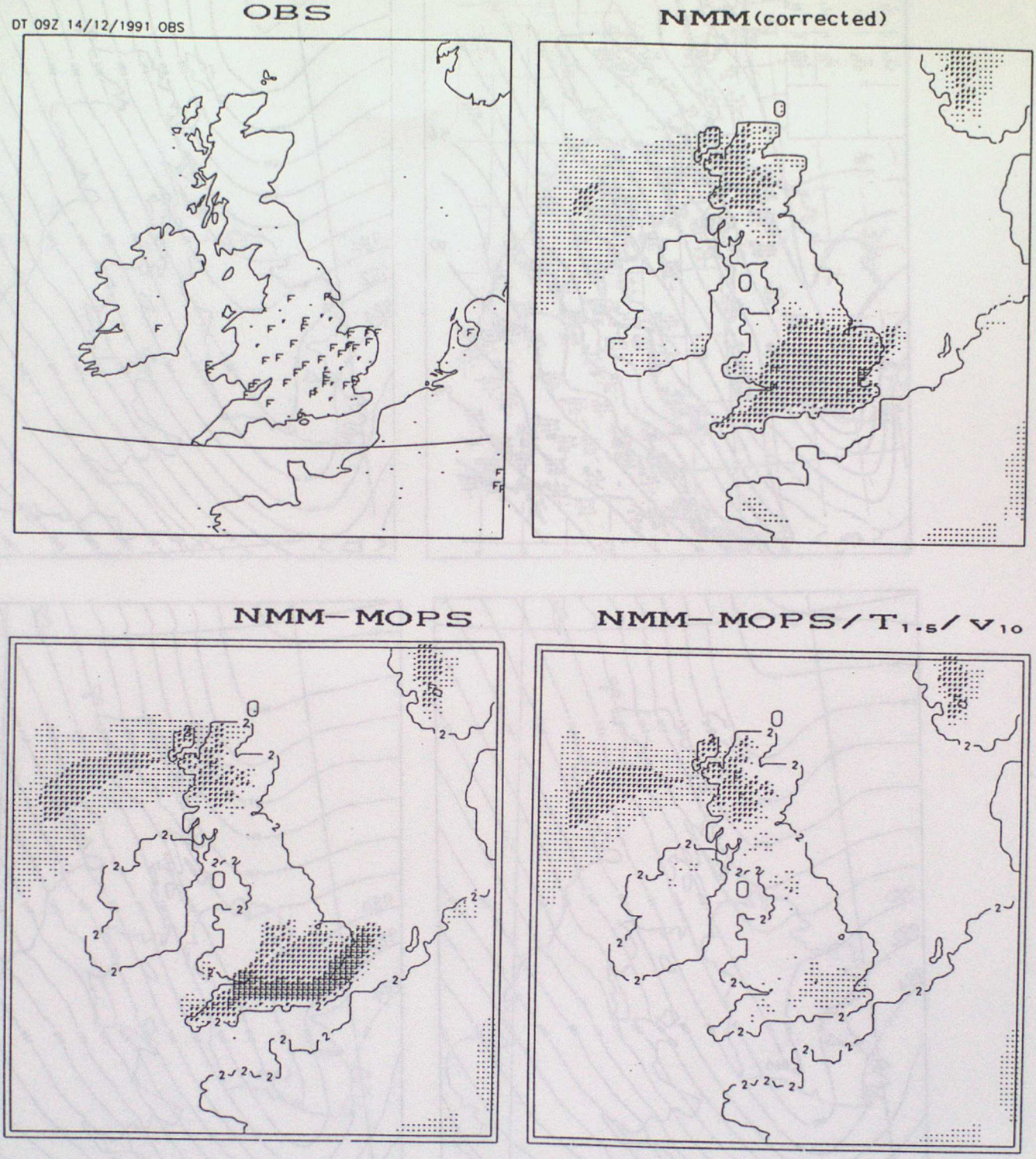

FIGURE 24: Observations and t+3 forecasts of visibility at 9z, 14/12/91. Symbols as in Figure 23.

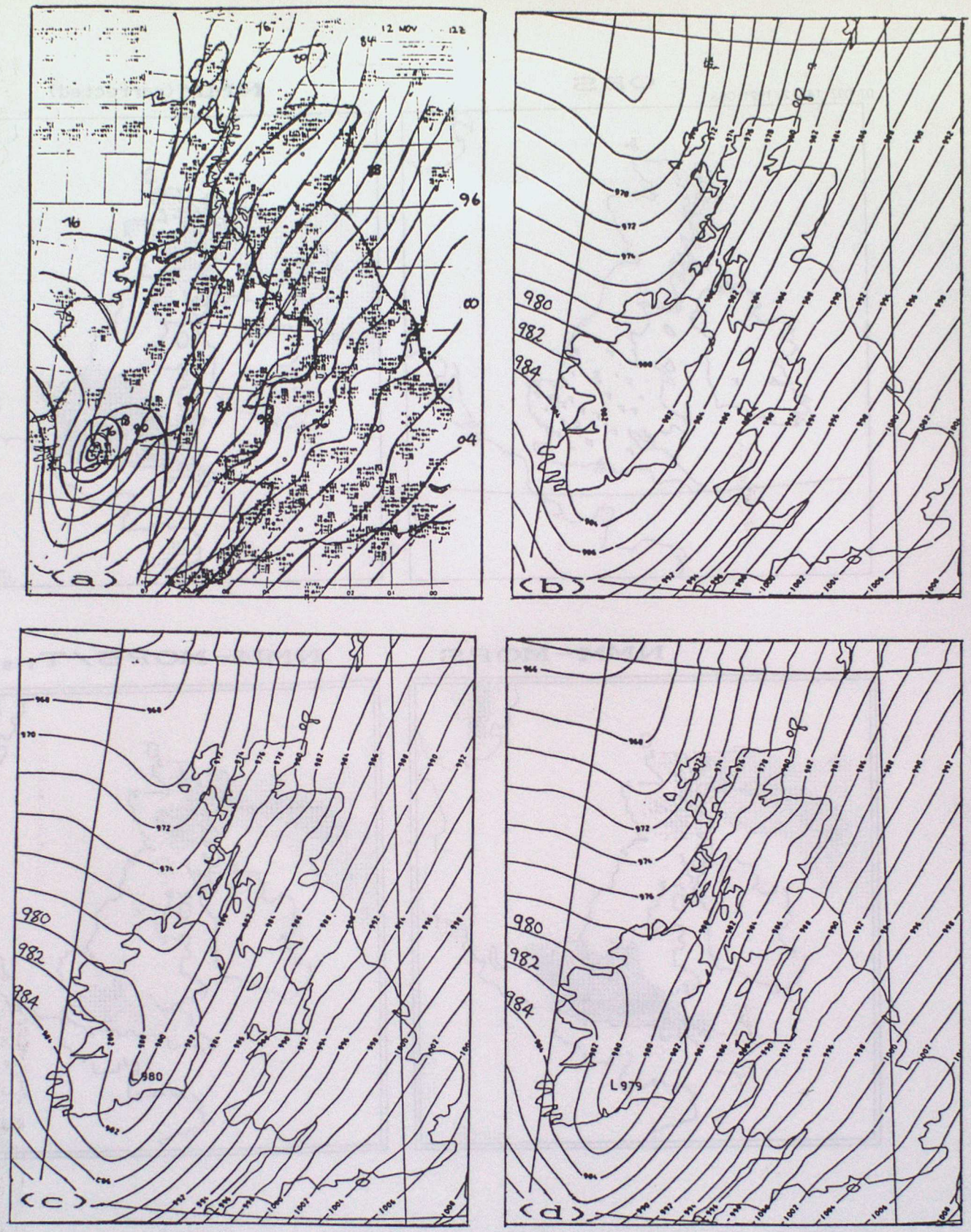

FIGURE 25: (a) surface analysis for 12z, 12/11/91
(b) t+0 from LAM
(c) t+0 from NMM with no synop wind data and 3-hourly surface pressure data
(d) t+0 from NMM *with* hourly synop wind and surface pressure data.

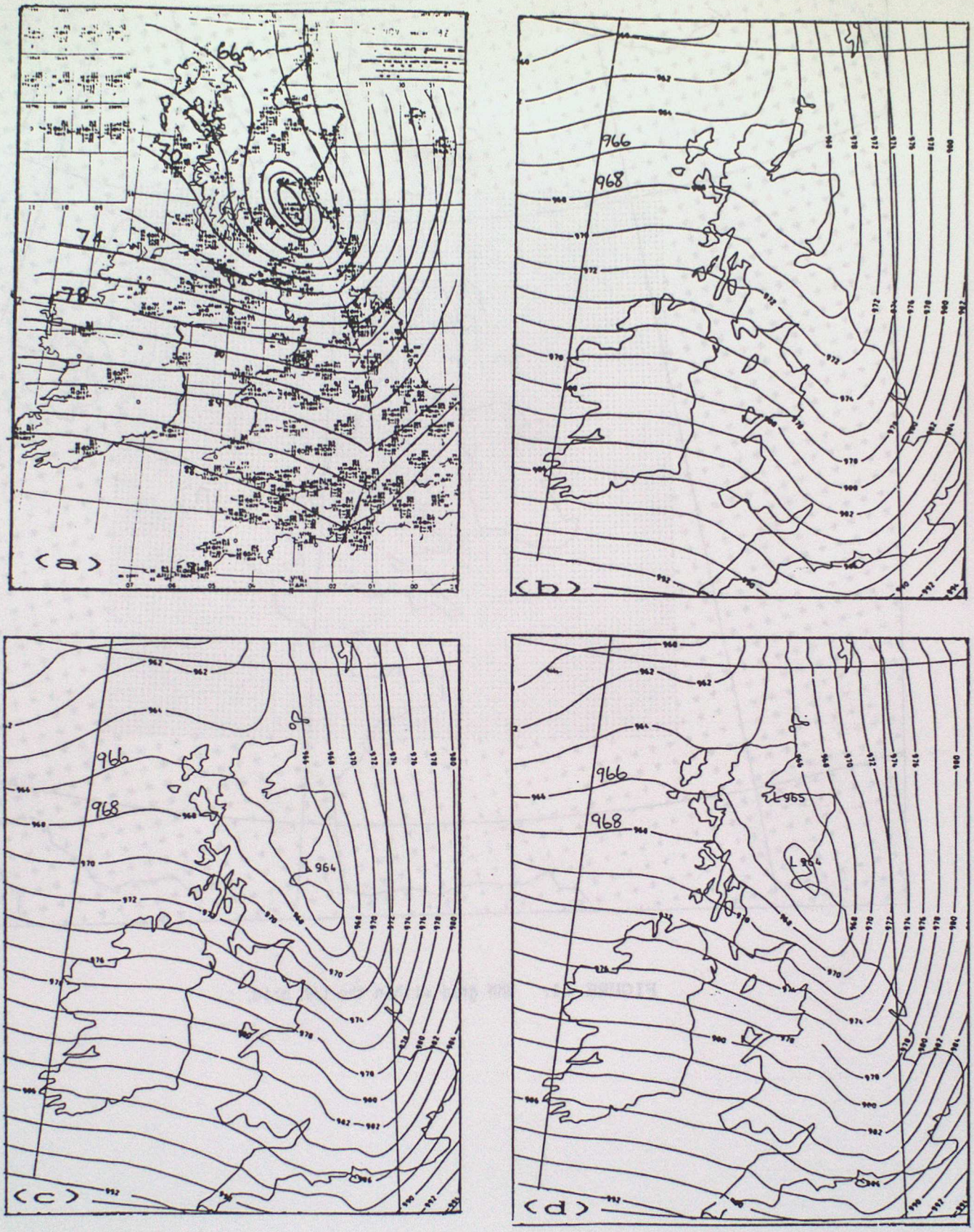

FIGURE 26: (a) surface analysis for 18z, 12/11/91
(b) t+6 from LAM
(c) t+6 from NMM with no synop wind data and 3-hourly surface pressure data
(d) t+6 from NMM *with* hourly synop wind and surface pressure data.

FIGURE A1: NMM grid within the LAM grid.

GEOPOTENTIAL HEIGHT
VALID AT 0.01Z ON 14/11/1992 DAY 319 DATA TIME 0Z ON 14/11/1992 DAY 319
SURFACE

FIGURE A2: NMM orographic height, with contours at 100m intervals. The coastline is indicated by the 1m contour.

FIGURE A3: Full levels (_____) and half-levels (- - -) of the operational NMM

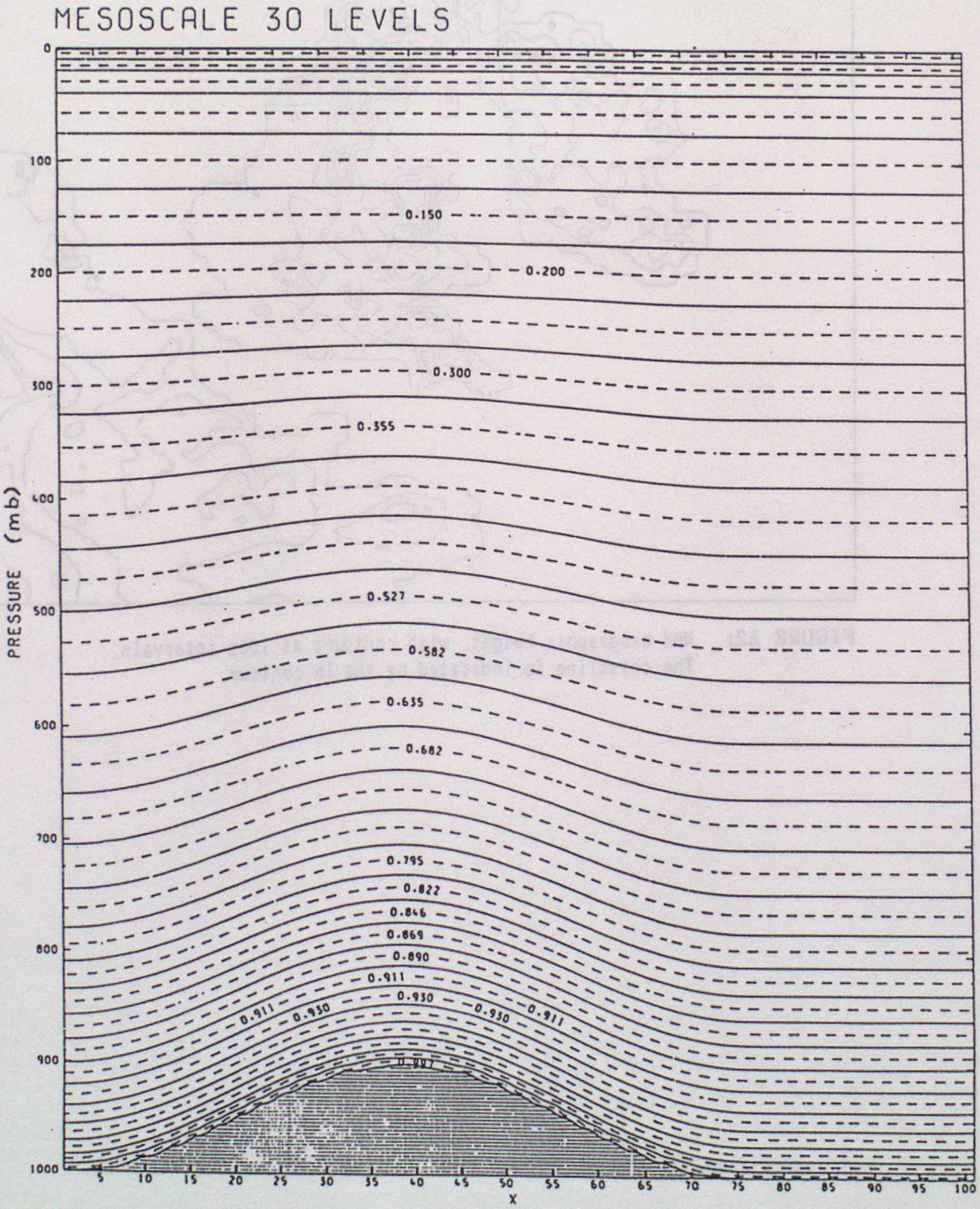

FIGURE A4: Model Level Heights (m)

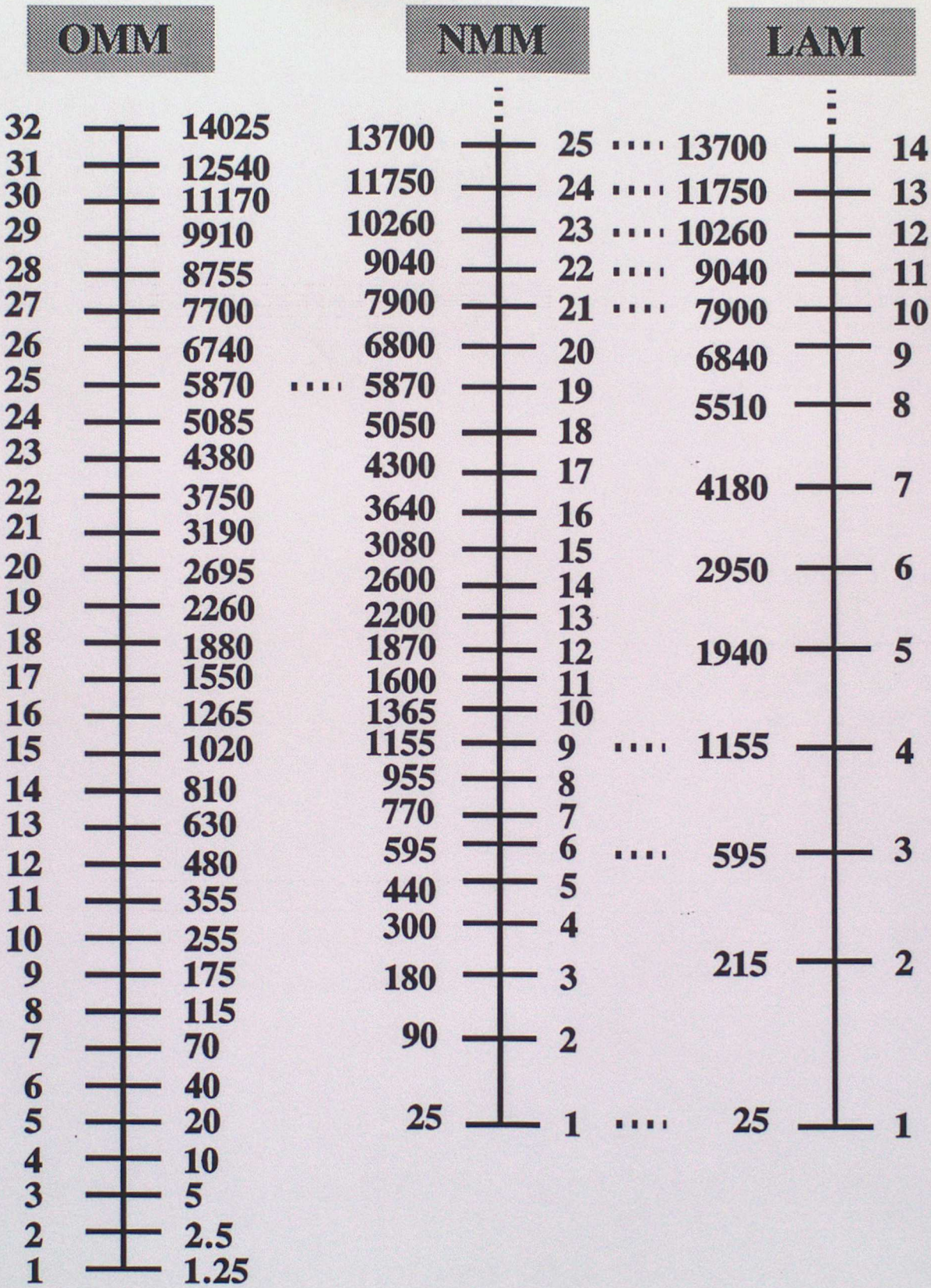

Forecasting Research Division Technical Reports

1.	ON THE TIME SAVING THAT CAN BE ACHIEVED BY THE USE OF AN OPTIMISED COURSE IN AN AREA OF VARIABLE FLOW	R.W. Lunnon A.D. Marklow September 1991
2.	Treatment of bias in satellite sea surface temperature observations	R.S.Bell August 1991
3.	FINITE DIFFERENCE METHODS	M.J.P. Cullen August 1991
4.	Representation and recognition of convective cells using an object-orientated approach	W.H. Hand 30th September 1991
5.	Sea-ice data for the operational global model.	C.P.Jones November 1991.
6.	Tuning and Performance of the Atmospheric Quality Control.	N.B. Ingleby. December 1991.
7.	More satellite sounding data - can we make good use of it?	R.S.Bell January 1992.
8.	WAM/UKMO Wind Wave model Intercomparison Summary Report	Heinz Gunther ECMWF Martin Holt UK Met Office January 1992
9.	Spin up problems of the UKMO Mesoscale Model and moisture nudging experiments	Akihide Segami JMA February 1992
10.	A comparison of 2nd generation and 3rd generation wave model physics	M.W. Holt B.J. Hall February 1992
11.	RETRIEVAL AND ASSIMILATION: SYSTEM CONSIDERATIONS	Andrew C Lorenc March 1992
12.	Detection of Precipitation by Radars in the UK Weather Radar Network	M. Kitchen P.M. Brown April 1992
13.	THE VALUE OF WIND OBSERVATIONS FOR WEATHER FORECASTING AND CLIMATE STUDIES	Andrew C Lorenc April 1992
14.	An investigation into the parameters used in the analysis scheme of the Mesoscale Model	G. Veitch B.J. Wright S.P Ballard May 1992
15.	THE VERIFICATION OF MESOSCALE MODEL FORECASTS OF LIQUID WATER CONTENT USING HELICOPTER REPORTS OVER THE NORTH SEA DURING WINTER 1991	M. Ahmed R.W Lunnon R.J. Graham May 1992

Forecasting Research Division Technical Reports

16.	Simulations of the Diurnal Evolution of Marine Stratocumulus Part I: The sensitivity of the Single Column Version of the Mesoscale Model to Changes in the Turbulence Scheme.	S.D.Jackson S.P. Ballard May 1992
17.	Simulations of the Diurnal Evolution of Marine Stratocumulus Part II: A Comparison of Radiation Schemes Using the Single Column Version of the Mesoscale Model.	S.D.Jackson S.P. Ballard May 1992
18.	Quantifying the low level windshear aviation hazard for the UK: some research proposals	R.J. Graham R.W. Lunnon May 1992
19.	WAM/UKMO Wind Wave model Intercomparison Part 2 Running the UKMO wave model at higher resolution	M.W. Holt April 1992
20.	Sensitivity of Mesoscale Model forecasts of anticyclonic Statocumulus to the specifications of initial conditions and Boundary Layer mixing scheme.	B.J. Wright S.P. Ballard July 1992
21.	Evaluation of diffusion and gravity wave changes in the Global Forecast Model.	F. Rawlins O. Hammon 16 June 1992
22.	Background Errors for the Quality Control and Assimilation of Atmospheric Observations in the Unified Model - the situation in July 1992.	C.A. Parrett July 1992
23.	Estimation of the Mean and Standard Deviation of the Random Component of Data also Containing Non- random Errors.	B.R. Barwell July 1992
24.	Experiments in Nowcasting convective rain using an object- oriented approach.	W.H. Hand 15th August 1992
25.	Gravity Wave Speeds from the Eigenmodes of the Unified	I. Roulstone 28 July 1992
26.	A re-calibration of the Wave Model	M.W. Holt August 1992
27.	Evaluation of Koistinen's method of radar range and bright band correction	A.G. Davies August 1992
28.	A Study of the Boundary Layer in the Mesoscale Unified Model	Graham Veitch August 21,1992
29.	Profiles of wind using time-sequences of absorption channel imagery from geostationary satellites: proof of concept using synthetic radiances	R.W.Lunnon September 1992
30.	AN EMPIRICAL INVESTIGATION OF THE "WATER VAPOUR TEMPERATURE LAPSE-RATE FEEDBACK" TO THE GREENHOUSE EFFECT	K.F.A. Smith R.J. Allam J.S.Foot September 1992
31.	Observation needs for operational ocean modelling	S.J. Foreman September 1992

Forecasting Research Division Technical Reports

32.	Bright band correlations for layered precipitation; the comparison of Chilbolton radar data and Hardaker model output.	A.G. Davies November 1992
33.	Progress and performance of the operational mesoscale model	S.P. Ballard
34.	Assessment of the bias of significant wave height in the Met.Office global wave model	S.J. Foreman M.W. Holt S. Kelsall
35.	STUDY OF CIRRUS CLOUD WINDS: ANALYSIS OF I.C.E DATA FINAL REPORT FOR EUMETSAT CONTRACT ITT 91/16	R.W. Lunnon D.A. Lowe J.A. Barnes I. Dharssi December 1992
36.	Revisions to the operational data assimilation-Nov.92	R.S. Bell January 1993
37.	A comparison of wind observations from a flight of the DRA(B)BAC 1-11 research aircraft over Hemsby, 11 June 1991, with observations from the Hemsby radiosonde	R.J. Graham January 1993
38.	The Moisture Observation Pre-processing System	B.J. Wright January 1993
39.	Performance of the data assimilation scheme in the operational trial of the new mesoscale model.	B. Macpherson B.J. Wright A.J. Maycock January 1993
40.	Development and performance of the new mesoscale model.	S.P. Ballard B. Robinson January 1993